RESEARCH ARTICLE

Two new species of *Dixonius* from Vietnam and Laos with a discussion of the taxonomy of *Dixonius* (Squamata, Gekkonidae)

Vinh Quang Luu[1,2], Thuong Huyen Nguyen[1], Minh Duc Le[3,4,5], Jesse L. Grismer[2], Hong Bich Ha[6], Saly Sitthivong[7], Tuoi Thi Hoang[1], L. Lee Grismer[2,8]

1 *Faculty of Forest Resources and Environmental Management, Vietnam National University of Forestry, Xuan Mai, Chuong My, Hanoi, Vietnam* **2** *Herpetology Laboratory, Department of Biology, La Sierra University, 4500 Riverwalk Parkway, Riverside, California 92505, USA* **3** *Faculty of Environmental Sciences, University of Science, Vietnam National University, Hanoi, 334 Nguyen Trai Road, Hanoi, Vietnam* **4** *Central Institute for Natural Resources and Environmental Studies, Vietnam National University, Hanoi, 19 Le Thanh Tong, Hanoi, Vietnam* **5** *Department of Herpetology, American Museum of Natural History, Central Park West at 79th Street, New York, New York 10024, USA* **6** *College of Forestry Biotechnology, Vietnam National University of Forestry, Hanoi, Vietnam* **7** *Faculty of Forestry, National University of Laos, Dong Dok Campus, Vientiane, Lao PDR* **8** *Department of Herpetology, San Diego Natural History Museum, PO Box 121390, San Diego, California, 92112, USA*

Corresponding authors: Vinh Quang Luu (vinhlq@vnuf.edu.vn); L. Lee Grismer (lgrismer@lasierra.edu)

Citation: Luu VQ, Nguyen TH, Le MD, Grismer JL, Ha HB, Sitthivong S, Hoang TT, Grismer LL (2023) Two new species of *Dixonius* from Vietnam and Laos with a discussion of the taxonomy of *Dixonius* (Squamata, Gekkonidae). ZooKeys 1163: 143–176. https://doi.org/10.3897/zookeys.1163.101230

Abstract

Integrated analyses using maximum likelihood (ML), Bayesian inference (BI), principal component analysis (PCA), discriminate analysis of principal components (DAPC), multiple factor analysis (MFA), and analysis of variance (ANOVA) recovered two new diagnosable species of gekkonid lizards in the genus *Dixonius*, one from the Central Highlands, Gia Lai Province, Vietnam and another from the Vientiane Province, Laos. Phylogenetic analyses based on the mitochondrial NADH dehydrogenase subunit 2 gene (ND2) and adjacent tRNAs showed that *Dixonius gialaiensis* **sp. nov.** is the sister species of *D. minhlei* from Dong Nai Province, Vietnam and is nested within a clade that also includes the sister species *D. siamensis* and *D. somchanhae*. *Dixonius muangfuangensis* **sp. nov.** is the sister species to *D. lao* from Khammouane Province, Laos and is embedded in a clade with *D. vietnamensis*, *D. taoi*, and undescribed species from Thailand. Multivariate (PCA, DAPC, and MFA) and univariate (ANOVA) analyses using combina-

tions of 15 meristic (scale counts), six morphometric (measurements), and five categorical (color pattern and morphology) characters from 44 specimens encompassing all eight species of *Dixonius* from Vietnam and Laos clearly illustrate *Dixonius gialaiensis* **sp. nov.** and *Dixonius muangfuangensis* **sp. nov.** are statistically different and discretely diagnosable from all closely related species of *Dixonius*. These integrative analyses also highlight additional taxonomic issues that remain unresolved within *Dixonius* and the need for additional studies. The discovery of these new species further emphasizes the underappreciated herpetological diversity of the genus *Dixonius* and illustrates the continued need for field work in these regions.

Introduction

The genus *Dixonius* was established by Bauer et al. (1997) to contain two species, *D. melanostictus* (Taylor, 1962) and *D. siamensis* (Boulenger, 1898), with a distribution range through Myanmar, Thailand, Laos, Vietnam, and Cambodia. Currently, thirteen species have been recognized worldwide (Nguyen et al. 2020, 2021; Pauwels et al. 2021; Uetz et al. 2022). In Vietnam, six species of *Dixonius* have been documented, including four originally described from the country, i.e., *D. vietnamensis* (Das 2004) from Khanh Hoa and Binh Thuan provinces, *D. aaronbaueri* (Ngo and Ziegler 2009) from Ninh Thuan and Binh Thuan provinces, *D. taoi* (Botov, Phung, Nguyen, Bauer, Brennan & Ziegler, 2015) from Binh Thuan Province, *D. minhlei* (Ziegler, Botov, Nguyen, Bauer, Brennan, Ngo & Nguyen, 2016) from Dong Nai Province, and two from outside Vietnam, *D. siamensis* from Thailand and Cambodia and *D. melanostictus* from Thailand (Uetz et al. 2022). Lastly, in Laos, there are three species (*D. siamensis*, *D. lao* (Nguyen, Sitthivong, Ngo, Luu, Nguyen, Le & Ziegler, 2020), *D. somchanhae* (Nguyen, Luu, Sitthivong, Ngo, Nguyen, Le & Ziegler, 2021)) two of which, *D. lao* from Vientiane Capital and *D. somchanhae* from Khammouane Province, were described within the last five years (Fig. 1).

During a recent herpetofaunal surveys in Chu Se Mountain Pass, Hbong Commune, Gia Lai Province in Vietnam and Vientiane Province in Laos, new populations of *Dixonius* were found at each location (Fig. 1). Based on phylogenetic evidence from the mitochondrial NADH dehydrogenase subunit 2 (ND2) gene and adjacent tRNAs, morphometric, meristic, and color pattern data, neither can be ascribed to any known species and as such they are described below as new species.

Materials and methods

A total of six *Dixonius* specimens were caught by hand from Gia Lai Province, Vietnam and Vientiane Province, Laos. The specimens were fixed in approximately 80% ethanol and then transferred to 70% ethanol for permanent storage. Tissue samples taken before the specimens were preserved were stored separately in 95% ethanol.
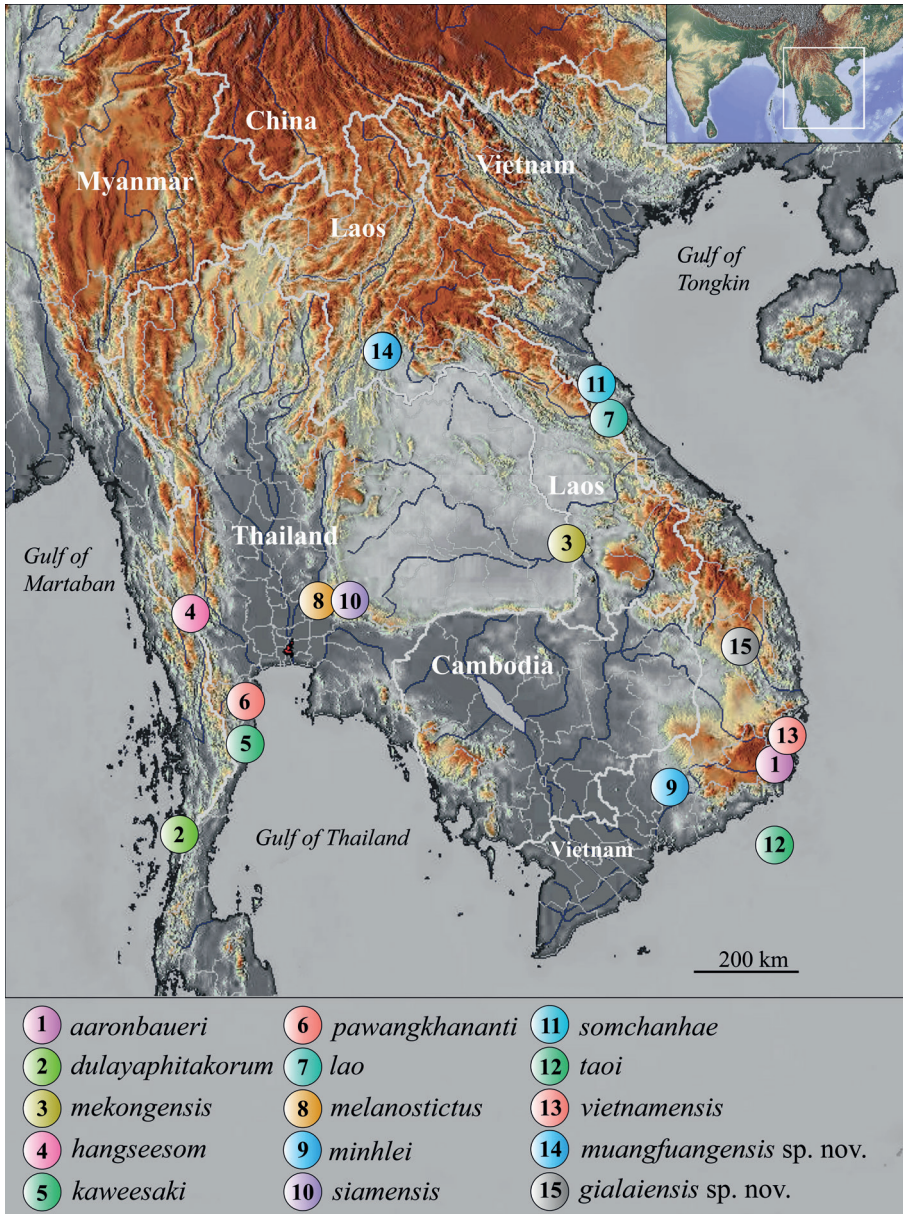
Figure 1. Location of the type localities of all known species of *Dixonius*. The inset delimits the study area. **1** *Dixonius aaronbaueri* from Ninh Thuan Province, Vietnam; **2** *D. dulayaphitakorum* from Ranong Province, Thailand; **3** *D. mekongensis* from Ubon Ratchathani Province, Thailand; **4** *D. hangseesom* from Kanchanaburi Province, Thailand; **5** *D. kaweesaki* from Prachuap Khiri Khan Province, Thailand; **6** *D. pawangkhananti* from Phetchaburi Province, Thailand; **7** *D. lao* from Khammouane Province, Laos; **8** *D. melanostictus* from Nakhon Ratchasima Province, Thailand; **9** *D. minhlei* from Dong Nai Province, Vietnam; **10** *D. siamensis* from SaraBuri and Nakhon Ratchasima provinces, Thailand; **11** *D. somchanhae* from Vientiane Capital, Laos; **12** *D. taoi* from Binh Thuan Province, Vietnam; **13** *D. vietnamensis* from Khanh Hoa Province, Vietnam; **14** *D. muangfuangensis* sp. nov. from Vientiane Province, Laos; **15** *D. gialaiensis* sp. nov. from Gia Lai Province, Vietnam.

The specimens have been deposited in the collection of the Vietnam National University of Forestry (**VNUF**), Hanoi, Vietnam and the National University of Laos (**NUOL**), Vientiane, Laos.

Species delimitation

The general lineage concept (GLC: de Queiroz 2007) adopted herein proposes that a species constitutes a population of organisms evolving independently from other such populations owing to a lack of, or limited gene flow. By "independently," it is meant that new mutations arising in one species cannot spread readily into another species (Barraclough et al. 2003; de Queiroz 2007). Molecular phylogenies recovered multiple monophyletic mitochondrial lineages of individuals (populations) that were used to develop initial species-level hypotheses, the grouping stage of Hillis (2019). Discrete color pattern data and univariate and multivariate analyses of morphological data were then used to search for characters and morphospatial patterns consistent with the tree-designated species-level hypotheses, the construction of boundaries representing the hypothesis-testing step of Hillis (2019), thus providing independent diagnoses to complement the molecular analyses. In this way, delimiting (phylogeny) and diagnosing (taxonomy) species are not conflated (Frost and Hillis 1990; Frost and Kluge 1994; Hillis 2019).

Molecular data and phylogenetic analyses

Four samples of the newly collected specimens were analyzed, two from Gia Lai Province, Vietnam (VNUF R.2020.22 – field number GL.02, VNUF R.2020.33 – field number GL.03) and two from Vientiane Province, Laos (VNUF R.2022.42 – field number MF.02, VNUF R.2022.52 – field number MF.03). We used the protocols of Nguyen et al. (2021) for DNA extraction, amplification, and sequencing. The complete NADH dehydrogenase subunit 2 (ND2) gene with six partial or complete adjacent tRNAs, approximately 1200 bp long, respectively, were amplified and sequenced using the primer pair, MetF1(5'-AAGCTTTCGGGCCCATACC-3') and COIR1(5'-AGRGTGCCAATGTCTTTGTGRTT-3') (Macey et al. 1997). Genomic DNA was extracted from all liver tissues stored in ethanol following the standard protocols of DNeasy blood and tissue kit, Qiagen (California, USA). The PCR volume consisted of 20 μl (1 μl each primer, 7 μl water, 10 μl of Taq mastermix and 1 μl DNA template). PCR conditions were: 95 °C for 5 min, followed by 42 cycles: 95 °C for 30 s, 50 °C for 45 s and 72 °C for 60 s with a final elongation step for 6 min at 72 °C. PCR products were visualized using electrophoresis through a 1.2% agarose gel, marker 100 bp, 1X TAE and stained with RedSafe Nucleic Acid Staining Solution and photographed under UV light of Geldoc system (Quantum CX5, Villber, France). Successful amplifications were purified using innuPREP Gel Extraction Kit (Analytik Jena, Germany). Cleaned PCR products were sent to 1st Base (Malaysia) for sequencing in both directions.

　　We obtained 1,444 base pairs of NADH dehydrogenase subunit 2 gene (ND2) sequence data and the flanking tRNAs from 29 ingroup individuals of *Dixonius*

representing 13 nominal species including the new samples from Vietnam and Laos. *Heteronotia spelea* was used as an outgroup to root the tree based on the phylogenetic results generated by Gamble et al. (2015). Sequence data for other species were acquired from GenBank. Newly generated sequences were deposited in GenBank (Table 1).

Maximum likelihood (ML) and Bayesian inference (BI) were used to estimate phylogenetic trees. Best-fit models of evolution determined in IQ-TREE (Nguyen et al. 2015) using the Bayesian information criterion (BIC) implemented in ModelFinder (Kalyaanamoorthy et al. 2017) indicated that F81+F was the best-fit model of evolution for the tRNAMET and K2P+I, and HKY+F+G4 were the best models of evolution for tRNAs2 and ND2, respectively. The ML analysis was performed using the IQ-TREE webserver (Trifinopoulos et al. 2016) with 1000 bootstrap pseudoreplicates using the ultrafast bootstrap (UFB) analysis (Minh et al. 2013; Hoang et al. 2018). The BI analysis was performed on CIPRES Science Gateway (Miller et al. 2010) using MrBayes v. 3.2.4 (Ronquist et al. 2012). Two independent runs were performed using Metropolis-coupled Markov Chain Monte Carlo (MCMCMC), each with four chains: three hot and one cold. The MCMCMC chains were run for 80,000,000 generations with the cold chain sampled every 8000 generations and the first 10% of each run being discarded as burn-in. The posterior distribution of trees from each run was summarized using the sumt function in MrBayes v. 3.2.4 (Ronquist et al. 2012). Stationarity was checked with Tracer v. 1.6 (Rambaut et al. 2014) to ensure effective sample sizes (ESS) for all parameters were well above 200. We considered Bayesian posterior probabilities (BPP) of 0.95 and above and ultrafast bootstrap support values (UFB) of 95 and above as an indication of strong nodal support (Huelsenbeck et al. 2001; Minh et al. 2013). Uncorrected pairwise sequence divergences (p-distance) were calculated in MEGA 11 (Kumar et al. 2016) using the complete deletion option to remove gaps and missing data from the alignment prior to analysis.

A time-calibrated Bayesian phylogenetic tree was estimated using BEAST 2 (Bayesian Evolutionary Analysis by Sampling Trees) v. 2.7.3 (Drummond et al. 2012) implemented in CIPRES (Cyberinfrastructure for Phylogenetic Research; Miller et al. 2010) where the ingroup node subtending the split between *Dixonius aaronbaueri* and the remaining species was given a 24.04 mya prior with an offset range of 20.23–27.68 mya following Gamble et al. (2015). The split between *Heteronotia* and *Dixonius* was set at 45.0 mya with an offset range of 33.3–56.8 mya (Gamble et al. 2015). An input file was constructed in BEAUti (Bayesian Evolutionary Analysis Utility) v. 2.7.3. An optimized relaxed clock with unlinked site models, linked clock models and linked trees, and a calibrated Yule prior were employed for the species level. BEAST Model Test (Bouckaert and Drummond 2017), implemented in BEAST, was used to numerically integrate over the uncertainty of substitution models while simultaneously estimating phylogeny using Markov chain Monte Carlo (MCMC). MCMC chains were run for 80 million generations and logged every 8,000 generations. The BEAST log file was visualized in Tracer v. 1.7.2 (Rambaut et al. 2014) to ensure effective sample sizes (ESS) were above 200 for all parameters. A maximum clade credibility tree using mean heights at the nodes was generated using TreeAnnotator v. 2.7.3 (Rambaut and

Table 1. List of specimens used for the phylogenetic analyses.

Species	Catalog no.	Location	GenBank no.
Dixonius aaronbaueri	ZFMK87274	Nui Chua NP, Ninh Thuan Province, southern Vietnam	HM997152
Dixonius gialaiensis sp. nov.	VNUF R.2020.22 (Field no. GL.02)	Chu Se District, Gia Lai Province, Vietnam	OQ819041
	VNUF R.2020.33 (Field no. GL.03)	Chu Se District, Gia Lai Province, Vietnam	OQ8190412
Dixonius lao	VNUF R.2016.2	Khammouane Province, Laos	MT024681
	IEBR A.2019.5	Khammouane Province, Laos	MT024683
	IEBR A.2019.6	Khammouane Province, Laos	MT024682
Dixonius melanostictus	VU 022	Captive, Thailand	HM997153
Dixonius minhlei	ZFMK 97745	Vinh Cuu, Dong Nai Province, Vietnam	KX379194
Dixonius muangfuangensis sp. nov.	VNUF R.2020.42 (Field no. MF02)	Muangfuang District, Vientiane Province, Central Laos	OQ818586
	VNUF R.2020.52 (Field no. MF03)	Muangfuang District, Vientiane Province, Central Laos	OQ818587
Dixonius cf. *siamensis*	VU 023	Captive, Thailand	KX379195
Dixonius siamensis	LSUHC 7328	Phnom Aural, Purset Province, Cambodia	EU054299
	FMNH 263003	Keo Seima District, Mondolkiri- Province, Cambodia	EU054298
	LSUHC 7378	Phnom Aural, Purset Province, Cambodia	KP979732
Dixonius somchanhae	VNUF R.2020.2	Nasaithong District, Vientiane Capital, Laos	MW605166
	VNUF R.2020.1	Nasaithong District, Vientiane Capital, Laos	MW605165
	VNUF R.2020.3	Nasaithong District, Vientiane Capital, Laos	MW605167
	VNUF R.2020.55 (Field no. VT05)	Vientiane Capital, Laos	OQ818589
	VNUF R.2020.54 (Field no. VT04)	Vientiane Capital, Laos	OQ818588
	VNUF R.2020.59 (Field no.VT09)	Vientiane Capital, Laos	OQ818591
	VNUF R.2020.56 (Field no. VT0T06)	Vientiane Capital, Laos	OQ818590
Dixonius sp.	LSUHC 9466	Sai Yok, Kanchanaburi Province, Thailand	KX379196
Dixonius taoi	ZFMK 96680	Phu Quy Island, Binh Thuan Province, Vietnam	KP979733
	CAS 257300	Phu Quy Island, Binh Thuan Province, Vietnam	KP979734
	IEBR A 2014-26	Phu Quy Island, Binh Thuan Province, Vietnam	KP979735
	IEBR A 2014-27	Phu Quy Island, Binh Thuan Province, Vietnam	KP979736
Dixonius cf. *vietnamensis*	ZFMK 87273	Nui Chua, Ninh Thuan Province, Vietnam	KX379201
Dixonius vietnamensis	IEBR R.20163	Nha Trang, Khánh Hòa Province, Vietnam	KX379198

Drummond 2013) with a burn-in of the first 10% of each run. Nodes with Bayesian posterior probabilities (BPP) of 0.95 and above were considered strongly supported (Huelsenbeck et al. 2001; Wilcox et al. 2002).

Morphological data and analysis

The morphological data set comprised six closely related species including six type specimens of *Dixonius minhlei* from Dong Nai Province, Vietnam (IEBR A.0801-02, VNMN R.2016.1-2, ZFMK 97745-46), three type specimens of *D. lao* from Khammouane Province, Laos (VNUF R.2016.2, IEBR A.2016.5-6), eight specimens of *D. siamensis* from Pursat Province, Cambodia (LSUHC 07328, 07378, 08420, 08487,

08491, 08522, 09284, 09289), five type specimens of *D. somchanhae* from Vientiane Capital, Laos (VNUF R.2020.1-5), four specimens of *D.* sp. from Gia Lai Province, Vietnam, and 12 specimens of *D. vietnamensis* from Nha Trang Province, Vietnam (ZRC 2.6024-27, IEBR R.2016.1, 2016.3, 2016.4, VNMN R.2016.3-4, ZFMK 97747-49).

Morphological data included both meristic and morphometric characters. Morphological characters were taken from the 44 specimens following Bauer et al. (2004) and Ngo and Ziegler (2009). Morphometric characters were taken after preservation with a digital caliper to the nearest 0.1 mm under a zoom stereomicroscope on the right/left of the body. Recorded data included: **SVL**: snout-vent length (taken from the tip of the snout to the vent), **TaL**: tail length (taken from the vent to the tip of the tail, original or partially regenerated), **TW**: tail width (taken at the base of the tail immediately posterior to the postcloacal swelling), **BW**: body width (greatest width of torso, taken at the level of midbody), **HL**: head length (the distance from the posterior margin of the retroarticular process of the lower jaw to the tip of the snout), HW: head width (the distance from the posterior margin of the retroarticular process of the lower jaw to the tip of the snout), **HD**: head depth (the maximum height of head measured from the occiput to base of the lower jaw), **EL**: ear length (greatest oblique length across the auditory meatus), **TBL**: Tibia length (taken on the ventral surface from the posterior surface of the knee while flexed 90° to the base of the heel), **AG**: axilla to groin length (taken from the posterior margin of the forelimb at its insertion point on the body to the anterior margin of the hind limb at its insertion point on the body), **FA**: forearm length (taken on the ventral surface from the posterior margin of the elbow while flexed 90° to the inflection of the flexed wrist), **ED**: eye diameter (the greatest horizontal diameter of the eye-ball), **EN**: eye nostril distance (measured from the anterior margin of the bony orbit to the posterior margin of the external nares), **ES**: eye snout distance (measured from anteriormost margin of the bony orbit to the tip of snout), **EE**: eye ear distance (measured from the anterior edge of the ear opening to the posterior edge of the bony orbit), **IN**: internarial distance (measured between the external nares across the rostrum), **IO**: interorbital distance (measured between the dorsal-most edges of the bony orbits).

Meristic data taken were: **V**: ventral scales (counted transversely across the abdomen midway between limb insertions from one ventrolateral fold to the other), **DTR**: longitudinal rows of dorsal tubercles (counted transversely across the body midway between the limb insertions from one ventrolateral body fold to the other), **PV**: paravertebral scales (counted in a paravertebral row from first scale posterior to parietal scale to last scale at the level of vent opening), **PV'**: paravertebral scales (counted in a row between limb insertions), **T4**: lamellae under fourth toe (counted from the distal scale containing claw to basal scale that broadly contacts adjacent fragmented scales), **IOS**: Interorbital scales (counted at narrowest point between orbits), **ICS**: interciliary scales (counted between supraciliaries at midpoint of orbit), **SPL**: supralabials (counted from the largest scale at the corner of the mouth to the rostral scale), **IFL**: infralabials (counted from termination of enlarged scales at the corner of the mouth to the mental scale), **MO**: number of supralabial at midorbital position, **PP**: precloacal pores in males.

Color pattern on dorsum including the presence or absence of canthal stripes (**CanthStrp**), the presence or absence of strong darkly barred lips (**LipBar**), the presence or absence of dark-colored round blotches on the top of the head (**RdHdBlch**) and dorsum (**RdBodBlch**), and the presence or absence of two regularly arranged whitish tubercles on flanks (**Tub**). The raw morphological data for all characters and specimens are presented in Tables 2, 3.

All statistical analyses were performed using R v. 4.2.1 (R Core Team, 2021). Morphometric characters used in the statistical analyses were SVL, BW, HL, HW, HD, EL, ED, EN, ES, EE, IN, IO, FAr, TBLr, and AGr. Tail metrics were not used due to the high degree incomplete sampling (i.e., regenerated, broken, or missing). To remove potential effects of allometry on morphometric traits (sec. Chan and Grismer 2022), we used the following equation: $X_{adj} = \log(X) - \beta[\log(SVL) - \log(SVL_{mean})]$, where X_{adj} = adjusted value; X = measured value; β = unstandardized regression coefficient for each population; and SVL_{mean} = overall average SVL of all populations (Thorpe 1975, 1983; Turan 1999; Lleonart et al. 2000, accessible in the R package GroupStruct (available at https://github.com/chankinonn/ GroupStruct). The morphometrics of each species were normalized separately and then concatenated into a single data set so as not to conflate potential intra- with interspecific variation (Reist 1986; McCoy et al. 2006). All data were scaled to their standard deviation to ensure they were analyzed on the basis of correlation and not covariance. Meristic characters (scale counts) used in statistical analyses were SPLr/l, IFLr/l, MO, IOS, ICS, V, DTR, and T4r/l. Precloacal and femoral pores were omitted from the analyses due to their absence in females. Categorical characters analyzed were CanthStrp, LipBar, RdHdBlch, RdBodBlch, and Tub.

A Levene's test for normalized morphometric and meristic characters was conducted to test for equal variances across all groups. Analyses of variance (ANOVA) were conducted on meristic and normalized morphometric characters (see below) with statistically similar variances to search for the presence of statistically significant mean differences ($p < 0.05$) among species across the data set. Characters bearing statistical differences were subjected to a TukeyHSD test to ascertain which species pairs differed significantly from each other for those particular characters. Boxplots were generated for discrete meristic characters in order to visualize the range, mean, median, and degree of differences between pairs of species bearing statistically different mean values and violin plots were generated for continuous morphometric characters to visualize the same.

Morphospatial positions were visualized using principal component analysis (PCA) from the ADEGENET package in R (Jombart et al. 2010) to determine if their positioning was consistent with the putative species boundaries delimited by the molecular phylogenetic analyses and defined by the univariate analyses (see above). PCA, implemented using the "prcomp()" command in R, is an indiscriminate analysis plotting the overall variation among individuals (i.e., data points) while treating each individual independently (i.e., not coercing data points into pre-defined groups). Subsequent to the PCA, a discriminant analysis of principle components (DAPC) was used to test

Table 2. Sex and raw meristic and categorical data used in the analyses from specimens of *Dixonius* from Vietnam and Laos. m = male; f = female; j = juvenile; r/l = right/left.

Species	Museum no.	Sex	Meristic data						Categorical data				
			SPL r/l	IFL r/l	MO	IOS	V	T4 r/l	Canthal stripe	Lips strong barred	Blotches on the head round	Blotches on dorsum round	Two regularly disposed whitish tubercles on each side of the flanks
minhlei	IEBR A.0802	m	8	6	6	10	22	14	present	no	yes	yes	absent
	ZFMK 97746	m	8	6.5	6	10	23	14.5	present	no	yes	yes	absent
	IEBR A.0801	f	8.5	7	6	10	22	12	present	no	yes	yes	absent
	ZFMK 97745	f	7.5	6	5.5	10	23	13	present	no	yes	yes	absent
	VNMN R.2016.1	f	8	6	5.5	8	23	15	present	no	yes	yes	absent
	VNMN R.2016.2	f	8	6.5	6	7	20	13	present	no	yes	yes	absent
gialaiensis sp. nov.	VNUF R.2020.22	m	7.5	6	6	7	21	14	present	yes	yes	yes	present
	VNUF R.2020.33	f	7	6	6	7	19	14	present	yes	yes	yes	present
	VNUF R.2020.44	mj	8	7	6	7	21	14.5	present	yes	yes	yes	present
vietnamensis	ZRC 2.6024	m	5	6	5	10	20	13	present	no	no	no	present
	ZRC 2.6025	m	5	6	5	9	20	13	present	no	no	no	present
	ZRC 2.6026	j	5	6	6	8	20	13	present	no	no	no	present
	ZRC 2.6027	j	6	7	6	8	20	13	present	no	no	no	present
	IEBR R.2016.3	m	8	6	5.5	10	19	13.5	present	no	no	no	present
	VNMN R.2016.3	m	7.5	6	5.5	9	19	13.5	present	no	no	no	present
	IEBR R.2016.1	f	7	6	5.5	8	18	13.5	present	no	no	no	present
	VNMN R.2016.4	f	7.5	7	6	9	20	13	present	no	no	no	present
	ZFMK 97748	f	7.5	6	6	8	20	14	present	no	no	no	present
	ZFMK 97747	mj	7.5	6	5.5	10	15	13.5	present	no	no	no	present
	IEBR R.2016.4	f j	8	7	6	7	21	12.5	present	no	no	no	present
	ZFMK 97749	fj	7	6.5	5.5	8	19	13.5	present	no	no	no	present
sp.	VNUF R.2022.81	m	8	6.5	6	9	24	14	present	no	no	yes	present
	VNUF R.2022.82	f	7.5	5.5	6	8	23	14.5	present	no	no	yes	present
	VNUF R.2022.83	fj	8	7	6	8	23	14	present	no	no	yes	present
	VNUF R.2022.84	f j	8.5	6	6	8	22	13.5	present	no	no	yes	present
somchanhae	VNUF R.2020.3	m	7	5	6	8	24	14	present	yes	no	no	present
	VNUF R.2020.2	m	8	6	6	8	23	15	present	yes	no	no	present
	VNUF R.2020.1	m	8	5.5	6	8	23	15	present	yes	no	no	present
	VNUF R.2020.4	f	8	5.5	6	8	23	15	present	yes	no	no	present
	VNUF R.2020.5	f	8	6	6	7	26	13	present	yes	no	no	present
siamensis	LSUHC09284	f	8	7	6	9	19	14	absent	yes	no	yes	present
	LSUHC08522	f	8	6.5	6	10	22	14.5	absent	yes	no	yes	present
	LSUHC08487	f	8	7	6	10	20	14.5	absent	yes	no	yes	present
	LSUHC08420	m	8.5	7	6	10	21	13	absent	yes	no	yes	present
	LSUHC08491	f	8	7	6	9	20	14.5	absent	yes	no	yes	present
	LSUHC07328	j	7.5	6	5.5	9	22	14	absent	yes	no	yes	present
	LSUHC07378	m	8	6	6	10	20	14.5	absent	yes	no	yes	present
	LSUHC09289	m	7.5	6	6	10	21	16	absent	yes	no	yes	present
muangfuangensis sp. nov.	NUOL R.2022.01	m	7	6.5	6	7	21	15	absent	yes	no	no	present
	VNUF R.2020.42	m	8	7	6	7	20	15	absent	yes	no	no	present
	VNUF R.2020.52	f	8	6.5	6	7	21	15	absent	yes	no	no	present
lao	VNUF R.2016.2	m	9.5	8	7.5	9	23	15	absent	yes	no	no	absent
	IEBR A.2019.5	f	8.5	8	7	8	23	15	absent	yes	no	no	absent
	IEBR A.2019.6	f	9	7.5	8	8	24	15	absent	yes	no	no	absent

Table 3. Sex and raw morphometric data used in the analyses from specimens of *Dixonius* from Vietnam and Laos. m = male; f = female; j = juvenile.

Species	Museum no.	Sex	SVL	BW	HL	HW	HD	EL	ED	EN	ES	EE	IN	IO	FAr	TBLr	AGr
minhlei	IEBR A.0802	m	43.9	9.4	7.3	7.7	4.7	1.5	2.7	3.7	5	3.5	1.6	4	6.2	7.7	18.7
	ZFMK 97746	m	40.6	8.5	6.7	6	4.3	1.3	2.2	3.2	4.4	3.6	1.3	3.5	6.7	7	18.2
	IEBR A.0801	f	45.9	9.7	7.2	6.6	5.2	1.2	3.3	3.4	4.4	3.4	1.5	3.7	5.9	7.2	21.2
	ZFMK 97745	f	47.5	9.6	7.6	6.8	4.7	1.5	3.1	3.5	4.9	3.9	1.5	3.7	6	7.3	21.5
	VNMN R.2016.1	f	43.3	9.3	7.1	6.5	4.4	1.3	2.5	3.5	4.6	3.8	1.5	3.8	6.1	7.5	20.6
	VNMN R.2016.2	f	46.7	9.2	7.7	6.2	4.6	1.2	3.1	3.8	5.2	3.6	1.5	3.4	6.6	7	30.3
gialaiensis sp. nov.	VNUF R.2020.22	m	41.2	8.6	11.7	7.7	5.2	1.1	2.9	3.1	4.3	3.3	1.3	1.2	6.1	6.9	15.8
	VNUF R.2020.33	f	47.4	8.4	12.3	8.8	6.1	1.3	3.3	3.5	4.8	3.5	1.5	1.4	6.3	7.7	21.8
	VNUF R.2020.44	mj	35.9	8.3	10.9	6.8	4.7	0.9	2.6	2.9	3.8	3	1.3	1.3	4.5	5.6	14
vietnamensis	ZRC 2.6024	m	40.8	8	7.5	7.9	5.5	1	2.9	3.2	4.3	3.8	2.1	3.6	5.6	7.7	21
	ZRC 2.6025	m	42.4	9.1	7.5	7.6	6	1.1	2.9	3.7	4.6	4	1.6	3.6	6.2	7.2	21
	ZRC 2.6026	j	26.6	5.4	5.4	5.2	4	0.6	2.1	2.2	3	2.5	1.1	2.7	4.4	4.4	13
	ZRC 2.6027	j	25.9	4	5.2	5.1	3.3	0.6	1.8	2.3	3.5	2.2	0.9	2.1	4	4.6	11.8
	IEBR R.2016.3	m	39	6.5	6.9	6.8	4.2	1.1	2.8	2.9	3.9	3.1	1.1	1.6	4.7	6.5	14.8
	VNMN R.2016.3	m	39.9	7.8	7.2	7	4.7	0.8	2.5	3.4	4.6	3.3	1.3	1.7	5.2	6.5	16.6
	IEBR R.2016.1	f	43.5	7.6	7.6	6.9	4.7	1	2.7	3.1	4.5	2.7	1.3	1.6	5	6.2	19.2
	VNMN R.2016.4	f	43.7	8.6	7.7	7.7	4.7	1.1	2.8	3.4	4.7	3.6	1.3	1.8	5.5	6.3	18.2
	ZFMK 97748	f	45.2	10.3	8.5	8.2	5.7	1.3	2.9	3.8	5.4	4.3	1.5	2.7	5.5	6.6	19.2
	ZFMK 97747	mj	34.1	4.7	6.2	5.7	4.1	0.9	2.3	2.7	3.6	2.5	1.2	1.3	4.2	5.9	12.3
	IEBR R.2016.4	fj	31.2	5.2	5.7	5.8	3.7	0.9	2.4	2.4	3.4	2.4	1	1.2	3.1	4.8	11.9
	ZFMK 97749	fj	29.2	4.8	5.2	4.8	3.1	0.9	2.5	2.1	2.9	2.3	1	1.2	3.1	4.9	11.1
sp.	VNUF R.2022.81	m	46	10.7	13.7	7.8	5.7	1.4	2.2	3.4	4.8	3.7	1.7	1.9	5.5	6.8	20.2
	VNUF R.2022.82	f	35.2	7.5	10.9	6.9	3.3	1.1	2.1	2.9	4.1	3.2	1.3	1.6	4.7	6.2	14.2
	VNUF R.2022.83	fj	31.1	5.1	9.2	5.1	2.4	1.2	2.2	2.3	2.3	2.5	1.1	1.4	4.5	5.1	12.5
	VNUF R.2022.84	fj	30.3	5.6	9.3	5.8	3	0.8	2	2.7	3.4	2.9	1.1	1.5	3.7	4.6	13.3
somchanhae	VNUF R.2020.3	m	43.8	9.4	12.2	8.5	5.6	1.6	3.4	3	5.1	3.4	1.3	1.7	6.2	7.3	20.5
	VNUF R.2020.2	m	47.1	11.1	12.9	9.7	5.9	1.9	3.3	3.4	5	3.5	1.6	1.8	5.6	8	19.5
	VNUF R.2020.1	m	39.8	8.9	11.6	7.9	5.2	1.2	2.9	2.9	4.2	3.1	1.7	1.3	4.8	6.6	17.4
	VNUF R.2020.4	f	35.5	9.4	9.7	6.9	4.2	1.2	2.2	2.8	3.7	2.5	1.2	1.4	4.3	5.5	15.5
	VNUF R.2020.5	f	39.9	8.9	11.4	7.6	4.4	1.5	3.1	2.6	4	3.1	1.5	1.3	4.9	6	19.7
siamensis	LSUHC09284	f	45.4	8.6	12.8	8.7	5.2	1.6	3	3.7	5.1	4	2	3.6	6.7	7.3	19
	LSUHC08522	f	44.1	9.4	12.5	8.1	5.7	1.4	2.4	4.4	5.2	4.5	1.8	3.7	6.7	6.9	21.2
	LSUHC08487	f	48.6	10.7	14.3	8.7	5.4	1.6	3.2	3.4	5.4	4.2	1.7	3.5	7.1	8	21.8

Species	Museum no.	Sex	SVL	BW	HL	HW	HD	EL	ED	EN	ES	EE	IN	IO	FAr	TBLr	AGr
siamensis	LSUHC08420	m	46.9	8.8	13.1	9.1	5.3	1.3	2.7	3.7	5.3	3.9	1.5	3.7	6.7	7.3	20.7
	LSUHC08491	f	45.2	10.2	13	8.2	5.7	1.4	2.8	3.3	4.7	4.2	2	3.7	6.2	6.9	19
	LSUHC07328	j	28.6	5.8	8.4	5.5	3	0.7	2.1	2.4	3.3	2.8	1.5	2.8	3.8	5	12
	LSUHC07378	m	36.7	6.5	10.9	7.3	4.5	1.3	2.6	3.1	4.6	3.4	1.6	3.4	6	6.6	16.1
	LSUHC09289	m	45.3	9.1	12.7	8.6	5.1	1.6	2.6	3.7	5	3.6	2	3.5	7	7.3	18.9
muanghuangensis sp. nov.	NUOL R.2022.01	m	38.3	7.83	10.5	7.2	4.3	0.8	2.4	2.8	3	3.4	1.3	1.7	4.3	4.9	16.5
	VNUF R.2020.42	m	55.6	11.93	15.2	10.8	6.9	2.3	3	3.8	5.9	5.1	1.6	2.3	6.8	7.2	23.1
	VNUF R.2020.52	f	56.7	12.23	16.7	10.7	6.9	2.1	3.5	3.8	5.8	5.1	1.7	2.4	7.1	7.3	27.4
lao	VNUF R.2016.2	m	50.1	9.7	14.1	9.2	5.3	1.4	3.6	4.4	5.6	4.1	1.7	1.7	6.9	7.6	20.6
	IEBR A.2019.5	f	55.4	11.5	14.3	9.7	6.2	1.7	3.6	4	5.5	4.4	1.8	1.5	7.1	8.5	22.2
	IEBR A.2019.6	f	35.8	7.2	9.9	7	4	1.1	2.7	2.8	3.6	2.6	1.1	1.1	4.6	5.9	15.2

Table 4. Mean percentages of uncorrected pairwise sequence divergence (p-distances) among the species of *Dixonius*. Intraspecific p-distance are in bold font, n/a = data not applicable.

	Dixonius sp.	cf. *siamensis*	*aaronbaueri*	*taoi*	*vietnamensis*	cf. *vietnamensis*	*muanghuangensis* sp. nov.	*lao*	*minhlei*	*gidlaiensis* sp. nov.	*siamensis*	*somchanhae*	*melanostictus*
Dixonius sp.	**n/a**												
cf. *siamensis*	6.33	**n/a**											
aaronbaueri	18.52	18.37	**n/a**										
taoi	11.49	13.16	16.07	**0.01**									
vietnamensis	12.12	13.67	18.84	6.58.	**n/a**								
cf. *vietnamensis*	12.12	12.43	18.31	7.36	2.57	**n/a**							
muanghuangensis sp. nov.	10.78	8.17	18.17	11.36	12.79	12.50	**0.00**						
lao	8.46	9.26	16.66	10.90	11.90	11.39	3.10	**0.00**					
minhlei	13.97	15.33	17.56.	13.35	14.13	13.92	13.23	13.24	**n/a**				
gidlaiensis sp. nov.	13.51	14.27	15.73	11.78	13.40	13.18	13.11	10.90	3.60	**0.00**			
siamensis	13.71	14.83	16.14	11.74	12.33	12.22	12.70	11.96	12.54	10.56	**0.00**		
somchanhae	13.31	12.66	17.73	12.90	12.57	12.40	12.40	12.27	12.24	10.63	9.07	**0.00**	
melanostictus	13.30	13.04	15.16	11.23	13.12	13.01	11.99	10.70	14.09	11.53	12.10	11.09	**n/a**

for corroboration and further discrimination of morphospatial differences among the putative species. DAPC a priori groups the individuals of each predefined population inferred from the phylogeny into separate clusters (i.e., plots of points) bearing the smallest within-group variance that produce linear combinations of centroids having the greatest between-group variance (i.e., linear distance; Jombart et al. 2010). DAPC relies on standardized data from its own PCA as a prior step to ensure that variables analyzed are not correlated and number fewer than the sample size. Principal components with eigenvalues accounting for 90–95% of the variation in the data set were retained for the DAPC analysis according to the criterion of Jombart et al. (2010).

To test and further corroborate the PCA and DAPC analyses, we conducted a multiple factor analysis (MFA) on the above-mentioned morphological characters plus the categorical color pattern differences for a near total evidence data set (see Tables 5, 6). The MFA was implemented using the *mfa*() command in the R package FactorMineR (Husson et al. 2017) and visualized using the Factoextra package (Kassambara and Mundt 2017). MFA is a global, unsupervised, multivariate analysis that incorporates qualitative and quantitative data (Pagès 2015), making it possible to analyze different data types simultaneously in a nearly total evidence environment. In an MFA, each individual is described by a different set of variables (i.e., characters) which are structured into different data groups in a global data frame, in this case, quantitative data (i.e., meristics and normalized morphometrics) and categorical data (i.e., color pattern). In the first phase of the analysis, separate multivariate analyses are carried out for each set of variables, principal component analyses (PCA) for the quantitative data sets and multiple correspondence analysis (MCA) for categorical data. The data sets are then normalized separately by dividing all their elements by the square root of their first eigenvalues. For the second phase of the analysis, the normalized data sets are concatenated into a single matrix for a global PCA of the data. Standardizing the data in this manner prevents one data type from overleveraging another. In other words, the normalization of the data in the first phase prevents data types with the highest number of characters or the greatest amount of variation from outweighing other data types in the second phase. This way, the contribution of each data type to the overall variation in the data set is scaled to define the morphospatial distance between individuals as well as calculating each data type's and each character's contributions to the overall variation in the data set (Pagès 2015; Kassambara and Mundt 2017).

Results

Molecular results

The results of ML, BI, and BEAST analyses produced trees with identical topologies and strong support at nearly every node (Figs 2, 3). The molecular analyses suggest that *Dixonius aaronbaueri* is the sister species to a clade containing all other species of *Dixonius*. Additionally, all analyses recovered the newly discovered population from

Table 5. Summary statistics of the principal component analysis of *Dixonius* species. Abbreviations are listed in the Materials and methods.

	PC1	PC2	PC3	PC4	PC5	PC6	PC7
Standard deviation	3.01003227	1.685877698	1.23949927	1.189032683	1.136318219	0.950656207	0.922402779
Proportion of Variance	0.43144	0.13534	0.07316	0.06732	0.06149	0.04304	0.04052
Cumulative Proportion	0.43144	0.56678	0.63994	0.70727	0.76875	0.81179	0.85231
eigen	9.060294267	2.842183612	1.53635844	1.413798721	1.291219096	0.903747223	0.850826887
SVL	-0.183137642	0.011423135	-0.069418522	0.076025214	-0.119546371	0.451176774	-0.589642945
BW	-0.287276767	0.064974951	0.187163981	-0.199453201	0.019777911	-0.133068566	-0.114357041
HL	-0.222534372	0.251387029	0.23514022	0.300194841	0.119329084	-0.056134295	0.150350725
HW	-0.264923454	0.100856053	0.274888978	0.257153297	-0.193697896	-0.025433828	0.20364848
HD	-0.239223187	-0.126312635	0.224210506	-0.024761051	-0.413575793	0.029259717	0.233903564
EL	-0.2480955	0.169750915	0.178082873	0.002208353	0.210266124	0.137233441	-0.232577889
ED	-0.202876478	0.122593123	0.079950567	-0.239727042	-0.47584928	0.235373894	-0.048044975
EN	-0.265593548	-0.130857091	-0.293077474	0.03772842	0.029146276	-0.105240363	0.142115916
ES	-0.267303156	-0.128737264	-0.102433066	-0.036514974	-0.068578553	-0.009743264	0.195931987
EE	-0.276238196	-0.150072094	-0.016576264	0.149081788	0.006956725	-0.271219422	-0.084638951
IN	-0.239210846	-0.181935095	0.070874242	0.114696597	0.170327297	0.022503069	0.138746934
IO	-0.131045671	-0.460675273	-0.164479294	-0.032535496	0.242758327	-0.169473493	-0.152061581
FAr	-0.279019143	-0.171574811	-0.122828868	-0.090763378	0.096076353	-0.023168457	0.04857391
TBLr	-0.256167278	-0.099347048	-0.096744886	-0.219547386	0.043230096	0.332696024	0.101539921
AGr	-0.262180808	-0.1304743	0.000207287	-0.261650023	-0.044763987	-0.216118201	-0.26353247
SPLr.l	-0.138456955	0.383331303	-0.225322477	0.206591458	0.113507526	0.110869199	-0.176892801
IFLr.l	-0.089464182	0.168661032	-0.585083828	0.180041929	-0.237863864	-0.199925005	-0.127174583
MO	-0.156905954	0.393579439	-0.305813247	0.010226561	-0.089299256	-0.164453012	0.254918394
IOS	-0.068091843	-0.230600144	0.078301763	0.673617186	0.047911701	0.164434462	-0.062199104
V	-0.140473075	0.310134826	0.27924011	-0.11493361	0.255279707	-0.405751544	-0.23957707
T4r.l	-0.152382721	0.157971329	-0.130436885	-0.183960387	0.490226326	0.396201891	0.316382072

	PC8	PC9	PC10	PC11	PC12	PC13	PC14
Standard deviation	0.843138943	0.710443326	0.614017867	0.525772586	0.515133085	0.463343505	0.418149629
Proportion of Variance	0.03385	0.02403	0.01795	0.01316	0.01264	0.01022	0.00833
Cumulative Proportion	0.88616	0.91019	0.92815	0.94131	0.95395	0.96417	0.97249
eigen	0.710883277	0.50472972	0.37701794	0.276436812	0.265362095	0.214687204	0.174849113
SVL	0.265288193	-0.446853384	0.196416397	-0.110376596	0.139472173	-0.13673416	0.085656549
BW	0.09057594	-0.129906618	-0.173199899	0.177854897	0.108703018	-0.085524495	-0.103253386
HL	-0.070645969	-0.213980283	-0.087846741	-0.389903504	-0.321747003	-0.17842853	-0.021701889
HW	0.039378469	-0.022086396	0.070374143	0.022285485	0.134276418	-0.209651757	0.058151643
HD	0.139854316	-0.180680891	-0.127550531	0.157737189	-0.027411952	0.137530567	-0.134451774
EL	-0.203202698	0.278604397	-0.198153958	0.402630535	-0.109054652	-0.264792874	0.164044114
ED	-0.319474696	0.251272882	-0.008164379	0.059050615	-0.034208937	0.225488518	0.158104491
EN	0.295981088	0.09576584	0.048312128	0.019723407	0.172978909	0.06220716	-0.41905017
ES	0.426919556	0.259878689	-0.007215665	-0.131144367	0.25121175	-0.129629771	0.403591724
EE	0.038959782	-0.113710926	-0.227904855	0.339050813	-0.133303008	-0.064748891	-0.201696035
IN	-0.469863359	-0.267676841	-0.188020288	-0.317994993	0.412756086	0.253021631	0.111955286
IO	-0.122814373	0.056652546	-0.125361847	0.03792394	0.095742055	-0.182302581	0.359575483
FAr	-0.057154891	0.014271255	0.303625758	-0.210415667	-0.567849769	-0.191700829	-0.00332367
TBLr	-0.266800377	0.279797707	0.228807449	-0.14978157	0.145371473	-0.238209022	-0.413156342
AGr	0.069118103	0.008227511	-0.004079106	-0.18336757	-0.303043068	0.52714368	0.090386865
SPLr.l	0.178898959	0.359957261	-0.462995625	-0.293841774	0.004054536	0.173258047	-0.103413131
IFLr.l	-0.352501894	-0.193922056	0.002786908	0.157568267	0.04772871	-0.046397338	-0.113553524
MO	-0.000619521	-0.057816313	0.271775541	0.090085724	0.002030737	-0.003433238	0.40989474
IOS	-0.02790961	0.257813239	0.336314946	0.217437021	-0.064780745	0.352986111	0.03220845
V	-0.010841335	0.086524979	0.460243812	-0.002655612	0.309267431	0.129809552	-0.119165889
T4r.l	0.091314647	-0.276112686	0.005762572	0.333431445	-0.07395688	0.301989669	0.038025431

	PC15	PC16	PC17	PC18	PC19	PC20	PC21
Standard deviation	0.376199721	0.365477475	0.339179752	0.282916626	0.236187037	0.171149685	0.149480188
Proportion of Variance	0.00674	0.00636	0.00548	0.00381	0.00266	0.00139	0.00106
Cumulative Proportion	0.97923	0.98559	0.99107	0.99488	0.99754	0.99894	1
eigen	0.14152623	0.133573785	0.115042904	0.080041817	0.055784316	0.029292215	0.022344327
SVL	-0.083499418	0.052323475	-0.106015238	0.003344968	-0.031996278	0.03916795	-0.019457555
BW	-0.178247777	-0.058497317	0.597846907	-0.255954135	0.379366422	-0.199217481	0.221418054
HL	0.08265144	-0.13083192	-0.024132742	0.014837636	0.131660321	0.479388229	0.2891919
HW	0.244724903	-0.059011694	0.113956101	-0.074931386	0.04577337	-0.069612504	-0.732492773
HD	0.050630806	0.316234183	0.16660119	0.299515683	-0.49781424	0.046244883	0.219619924
EL	0.296740909	0.376559691	-0.260809485	-0.089676204	-0.027290387	-0.071210438	0.140852117
ED	-0.231235089	-0.168155577	-0.115371244	0.284151752	0.361474786	0.202917841	-0.049017145
EN	0.022603597	0.420837275	-0.236893263	0.02900181	0.436157574	0.238920063	-0.045962367
ES	0.248024801	-0.355459446	-0.140327076	0.068202164	0.014098586	-0.168841736	0.325882917
EE	-0.393037351	-0.425564191	-0.418495874	-0.066368342	-0.173649977	-0.04666024	-0.080329
IN	-0.081626216	0.152259274	-0.192312604	-0.041856001	0.036286384	-0.306664296	0.054524547
IO	-0.115305892	0.069986307	0.310505175	0.23842857	-0.096262685	0.459593261	-0.180632462
FAr	-0.116757716	0.126720851	0.055407627	0.30600813	0.081267972	-0.470097472	-0.064137815
TBLr	-0.021197578	-0.178071358	0.100589652	-0.310374261	-0.331807871	0.142300685	0.047913831
AGr	0.334353255	-0.016725971	-0.026314358	-0.397995653	-0.105887039	0.100382932	-0.137085205
SPLr.l	-0.184269598	0.036899566	0.194841372	0.163667167	-0.204455175	-0.121267207	-0.156153276
IFLr.l	0.428551026	-0.165166993	0.155004291	0.142458525	0.008969802	-0.065554124	0.111490515
MO	-0.391157106	0.255079755	-0.004834981	-0.342258191	-0.175496507	0.081476947	0.028734251
IOS	-0.059743664	-0.04851249	0.20733712	-0.095515858	0.057436279	-0.015186946	0.173384569
V	0.002458015	-0.062420243	-0.039680685	0.361422477	-0.145522506	0.02608135	0.040083497
T4r.l	0.117972701	-0.206198025	0.0622901	0.17118706	0.012651195	0.069479213	-0.122746338

Chu Se District, Gia Lai Province, Vietnam as the strongly supported (1.00/100) sister species of *D. minhlei* and the newly discovered population from Muangfuang District, Vientiane Province, Laos as the strongly supported (1.00/100) sister species of *D. lao* (Figs 2, 3). Uncorrected pairwise sequence divergences among *Dixonius* species ranged from 2.57–18.84% (Table 4). Ranges for the new species described (see below) are as follows: new species from Vietnam 3.60–15.73%, being most similar to *D. minhlei* and most distant to *D. aaronbaueri* and new species from Laos 3.10–18.17%, being most similar to *D. lao* and most distant to *D. aaronbaueri*.

The time-calibrated BEAST analysis places the divergence between *Dixonius aaronbaueri* and the remaining species of *Dixonius* at approximately 24.04 mya (20.23–27.68 highest posterior density [HPD]). Within the Vietnam's lineages, *D. gialaiensis* sp. nov. and *D. minhlei* diverged from each other at approximately 3.19 mya (0.79–5.78 HPD) and within the Lao lineages, *D. muangfuangensis* sp. nov. and *D. lao* diverged approximately 3.47 mya (1.37–6.16 HPD) (Fig. 3).

Statistical analyses

The first two principal components (PC1 and PC2) of the PCA analysis recovered 56.6% of the variation in the morphometric and meristic data set (Fig. 4A) and loaded most heavily for body width (BW), head width (HW), eye nostril distance (EN), eye snout distance (ES), and eye ear distance (EE) along PC1 and interorbital dis-
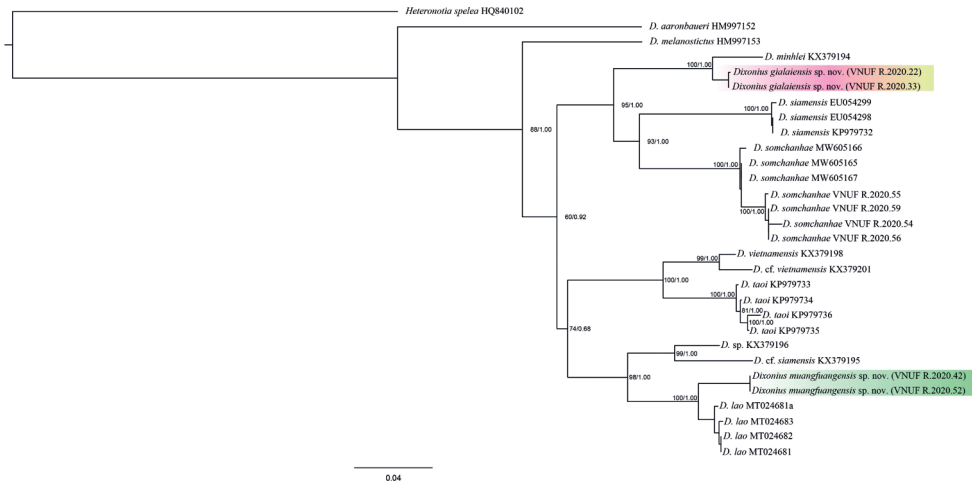
Figure 2. Maximum likelihood topology of the *Dixonius* species from Vietnam and Laos with ultrafast bootstrap values (UFB) and Bayesian posterior probabilities (BPP) at the nodes, respectively.
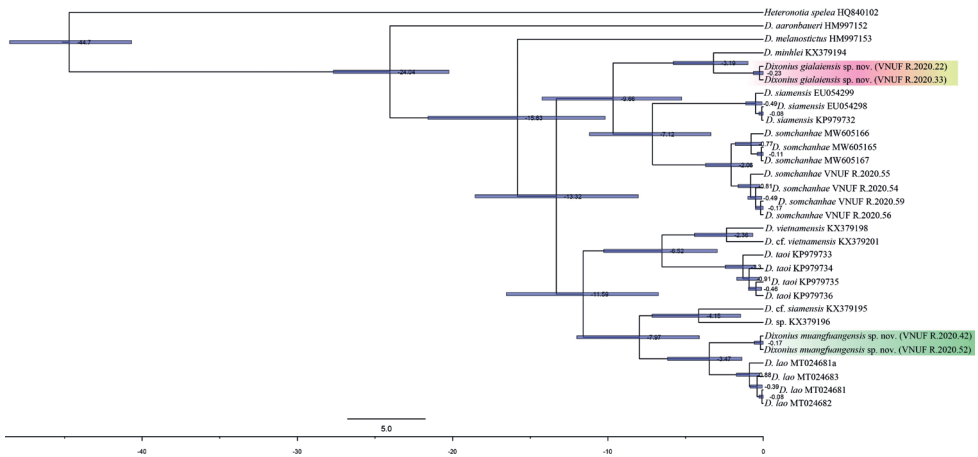

Figure 3. BEAST chronogram of the *Dixonius* species from Vietnam and Laos. Numbers at the nodes are mean ages in millions of years. Bars represent 95% highest posterior densities.

tance (IO), supralabials (SPLr/l), number of supralabial at midorbital position (MO), and ventral scales (V) along PC2 (Table 5). The PCA recovered *D. gialaiensis* sp. nov. and *D. muangfuangensis* sp. nov. to be widely separated from most other species with *D. muangfuangensis* sp. nov. only overlapping with the distantly related *D. siamensis*. The two distantly related new species are well-separated from most other species in the DAPC but each overlaps with one other species in their 67% inertia ellipses (Fig. 4B).

The MFA analysis recovered all species to be separated from one another including *Dixonius muangfuangensis* sp. nov. and *D. siamensis* (Fig. 5A). The morphometric data

Table 6. Summary statistics of morphometric and meristic characters among the *Dixonius* species.

Species	SVL	BW	HL	HW	HD	EL	ED	EN	ES	EE	IN	IO	FAr	TBLr	AGr	SPLr.l	IFLr.l	MO	IOS	V	T4r.l
Dixonius gialaiensis sp. nov. (*n* = 3)																					
Mean	1.62	0.93	1.07	0.89	0.73	0.04	0.47	0.50	0.63	0.51	0.14	0.11	0.75	0.83	1.23	7.5	6.33	6	7	20.33	14.17
SD	0.060	0.007	0.003	0.001	0.007	0.005	0.002	0.007	0.002	0.005	0.018	0.029	0.034	0.013	0.025	0.5	0.577	0	0	1.155	0.289
Lower	1.56	0.92	1.06	0.89	0.72	0.04	0.47	0.49	0.63	0.51	0.12	0.08	0.73	0.82	1.20	7	6	6	7	19	14
Upper	1.68	0.93	1.07	0.89	0.73	0.05	0.47	0.50	0.64	0.52	0.15	0.13	0.79	0.84	1.25	8	7	6	7	21	14.5
D. lao (*n* = 3)																					
Mean	1.67	0.98	1.11	0.94	0.71	0.15	0.52	0.57	0.69	0.57	0.18	0.16	0.79	0.87	1.29	9	7.83	7.5	8.33	23.33	15
SD	0.099	0.014	0.017	0.005	0.013	0.022	0.016	0.042	0.028	0.012	0.013	0.047	0.017	0.007	0.003	0.5	0.289	0.5	0.577	0.577	0
Lower	1.55	0.96	1.09	0.93	0.70	0.12	0.51	0.54	0.67	0.56	0.17	0.12	0.78	0.86	1.29	8.5	7.5	7	8	23	15
Upper	1.74	0.99	1.13	0.94	0.72	0.17	0.54	0.62	0.72	0.58	0.20	0.21	0.81	0.87	1.29	9.5	8	8	9	24	15
D. minhlei (*n* = 6)																					
Mean	1.65	0.97	0.86	0.82	0.67	0.12	0.45	0.55	0.68	0.56	0.17	0.57	0.80	0.86	1.33	7.75	6.42	5.83	7.67	21.33	14.33
SD	0.025	0.012	0.008	0.037	0.022	0.044	0.022	0.021	0.025	0.022	0.023	0.025	0.020	0.017	0.060	0.418	0.376	0.258	1.211	1.366	1.033
Lower	1.61	0.95	0.85	0.79	0.65	0.08	0.42	0.52	0.64	0.53	0.14	0.53	0.78	0.85	1.28	7	6	5.5	7	20	13
Upper	1.68	0.98	0.87	0.89	0.71	0.18	0.49	0.57	0.70	0.59	0.21	0.60	0.83	0.89	1.44	8	7	6	10	23	15
Dixonius muangfuangensis sp. nov. (*n* = 3)																					
Mean	1.69	1.03	1.15	0.99	0.78	0.21	0.47	0.54	0.68	0.66	0.19	0.33	0.78	0.81	1.35	8.17	6.5	6	10	22.33	13.5
SD	0.096	0.001	0.016	0.006	0.005	0.031	0.030	0.003	0.011	0.005	0.011	0.006	0.004	0.001	0.032	0.289	0.5	0	0	0.577	1.323
Lower	1.58	1.03	1.13	0.97	0.77	0.18	0.44	0.54	0.67	0.65	0.18	0.32	0.78	0.81	1.31	8	6	6	10	22	12
Upper	1.75	1.03	1.16	0.99	0.78	0.25	0.50	0.54	0.69	0.66	0.20	0.34	0.78	0.81	1.38	8.5	7	6	10	23	14.5
D. siamensis (*n* = 8)																					
Mean	1.62	0.93	1.09	0.90	0.70	0.13	0.43	0.54	0.68	0.58	0.25	0.54	0.80	0.84	1.27	7.94	6.56	5.94	9.63	20.63	14.38
SD	0.077	0.0357	0.009	0.014	0.029	0.048	0.034	0.044	0.021	0.031	0.046	0.016	0.028	0.017	0.021	0.320	0.496	0.177	0.518	1.061	0.835
Lower	1.61	0.95	0.85	0.79	0.65	0.08	0.42	0.52	0.64	0.53	0.14	0.53	0.78	0.85	1.23	7	6	5.5	7	20	13
Upper	1.68	0.987	0.87	0.89	0.71	0.18	0.49	0.57	0.70	0.59	0.21	0.60	0.83	0.89	1.44	8	7	6	10	23	15
D. somchanhae (*n* = 6)																					
Mean	1.62	0.97	1.07	0.91	0.70	0.17	0.46	0.48	0.65	0.50	0.18	0.23	0.73	0.83	1.26	7.75	5.67	6	8.17	23.33	14.67
SD	0.045	0.033	0.013	0.009	0.026	0.034	0.043	0.041	0.024	0.023	0.073	0.150	0.050	0.016	0.027	0.418	0.408	0	0.983	1.633	1.033
Lower	1.55	0.93	1.05	0.90	0.66	0.10	0.40	0.42	0.62	0.47	0.13	0.13	0.68	0.80	1.24	7	5	6	7	21	13
Upper	1.67	1.01	1.08	0.92	0.74	0.20	0.51	0.55	0.68	0.54	0.29	0.53	0.82	0.84	1.31	8	6	6	10	26	16

Species	SVL	BW	HL	HW	HD	EL	ED	EN	ES	EE	IN	IO	FAr	TBLr	AGr	SPLr.l	IFLr.l	MO	IOS	V	T4r.l
D. sp. (*n* = 4)																					
Mean	1.55	0.85	1.03	0.81	0.54	0.05	0.33	0.45	0.55	0.49	0.11	0.21	0.66	0.75	1.18	8	6.25	6	8.25	23	14
SD	0.083	0.033	0.009	0.037	0.049	0.068	0.017	0.033	0.087	0.033	0.007	0.015	0.032	0.032	0.020	0.408	0.645	0	0.5	0.816	0.408
Lower	1.48	0.81	1.02	0.76	0.49	-0.03	0.31	0.41	0.44	0.44	0.11	0.19	0.62	0.72	1.16	7.5	5.5	6	8	22	13.5
Upper	1.66	0.88	1.04	0.84	0.61	0.13	0.35	0.48	0.62	0.52	0.12	0.22	0.70	0.80	1.20	8.5	7	6	9	24	14.5
D. vietnamensis (*n* = 12)																					
Mean	1.56	0.83	0.83	0.82	0.65	-0.03	0.41	0.47	0.61	0.48	0.10	0.29	0.67	0.78	1.20	6.75	6.29	5.63	8.67	19.25	13.25
SD	0.088	0.055	0.016	0.028	0.049	0.054	0.030	0.031	0.035	0.055	0.070	0.165	0.063	0.035	0.051	1.177	0.450	0.377	0.985	1.545	0.399
Lower	1.41	0.72	0.80	0.77	0.58	-0.13	0.35	0.42	0.55	0.36	0.02	0.12	0.55	0.73	1.12	5	6	5	7	15	12.5
Upper	1.66	0.92	0.85	0.86	0.72	0.05	0.46	0.51	0.68	0.55	0.28	0.53	0.76	0.85	1.27	8	7	6	10	21	14

contributed to approximately 40% of the variation along Dim-1 followed by the categorical and meristic data. For Dim-2, the categorical data contributed 80% of the variation followed by morphometric and meristic data. Dim-3 showed that meristic data contributed 70% of the variation followed by morphometric and categorical data (Fig. 5B).

The ANOVAs and subsequent TukeyHDS tests demonstrated that *Dixonius gialaiensis* sp. nov. bears statistically different mean values between it and all other species in various combinations of characters (Tables 6, 7) and differs significantly from its sister species *D. minhlei* in head length (HL mean = 1.07 vs. 0.86, *p* = 0.000, respectively), in head width (HW mean = 0.89 vs. 0.82, *p* = 0.005, respectively), and in axilla to groin length, (AGr mean = 1.23 vs 1.32 *p* = 0.022) (Fig. 5; Tables 6, 7). *Dixonius muangfuangensis* sp. nov. also differed significantly from all other species in various combinations of characters and from its sister species *D. lao* it differs in head length (HL mean = 1.15 vs. 1.11, *p* = 0.004, respectively) and numbers of infralabials (IFL mean = 6.50 vs. 7.83, *p* = 0.026, respectively), and in numbers of supralabial at midorbital position (MO mean = 6.00 vs. 7.50, *p* = 0.00001, respectively) (Fig. 5, Tables 6, 7). Variation in all metric characters are visualized in Figs 6, 7.

Taxonomy

Dixonius gialaiensis sp. nov.
https://zoobank.org/10BF67E1-8059-47CE-891C-B219BD7AA9C1
Fig. 8
Gialai leaf-toed gecko

Material examined. *Holotype.* Adult male, VNUF R.2020.22 (Field no. GL02) in Chu Se Mountain Pass, H'Bong Commune, Chu Se District, Gia Lai Province (13°34'44.3"N, 108°13'55.7"E; 330 m a.s.l.), collected by Oanh Van Lo and Khanh Quoc Nguyen on 15 February 2020. *Paratypes.* VNUF R.2020.44 (Field No. GL04), juvenile male, and VNUF R.2020.33 (Field No. GL03), adult female; the same data as the holotype.

Diagnosis. *Dixonius gialaiensis* sp. nov. can be separated from all other species of *Dixonius* by possessing the unique combination of having a maximum SVL of 47.4 mm; 19 longitudinal rows of dorsal tubercles at midbody; 19–21 longitudinal rows of ventrals across the abdomen; 7 or 8 supralabials, sixth in at midorbital position; 6 or 7 infralabials; 7 interorbital scales; 7 or 8 precloacal pores in males, femoral pores lacking; precloacal and femoral pores absent in female; 13–15 lamellae on fourth toe; dorsum olive grey color with more round brown blotches; canthal stripe continues behind orbit to back of head; lips with dark bars; two regularly disposed whitish tubercles along the sides near the flanks to tail tip. These characters are scored across all *Dixonius* species from Vietnam and Laos in Tables 6, 7.

Description of the holotype. Adult male, SVL 41.2 mm; head moderate in length (HL/SVL 0.28), wide (HW/HL 0.66), depressed (HD/HL 0.44), distinct from

Table 7. Significant *p*-values from the results of the ANOVA and TukeyHDS analyses comparing all combinations of species pairs. Character abbreviations are listed in the Materials and methods.

Morphometric characters	BW	HL	HW	HD	EL	ED	EN	ES	FAr	TBLr	AGr
lao vs. *gialaiensis* sp. nov.		0.007									
minhlei vs. *gialaiensis* sp. nov.		0.00	0.005								0.022
muangfuangensis sp. nov. vs. *gialaiensis* sp. nov.	0.040	< 0.001	0.001		0.001						0.023
siamensis vs. *gialaiensis* sp. nov.											
somchanhae vs. *gialaiensis* sp. nov.					0.016						
sp. vs. *gialaiensis* sp. nov.		0.021	0.001	< 0.001		< 0.001				0.006	
vietnamensis vs. *gialaiensis* sp. nov.	0.005	0.00	< 0.001	0.030		0.040				0.036	
minhlei vs. *lao*		0.00	< 0.001			0.017					
muangfuangensis sp. nov. vs. *lao*		0.003									
siamensis vs. *lao*						< 0.001					
somchanhae vs. *lao*		< 0.001					0.002				
sp. vs. lao	0.002	< 0.001	< 0.001	< 0.001		< 0.001	< 0.001	< 0.001	0.005	< 0.001	0.018
vietnamensis vs. *lao*	< 0.001	0.00	< 0.001		< 0.001	< 0.001	< 0.001	0.017	0.001	< 0.001	0.023
muangfuangensis sp. nov. vs. *minhlei*		0.00	< 0.001	0.002							
siamensis vs. *minhlei*		0.00	< 0.001								
somchanhae vs. *minhlei*		0.00	< 0.001				0.006		0.035		
sp. vs. *minhlei*	< 0.001	0.00		< 0.001		< 0.001	0.001	< 0.001	< 0.001	< 0.001	< 0.001
vietnamensis vs. *minhlei*	< 0.001	< 0.001			< 0.001		< 0.001	0.007	< 0.001	< 0.001	< 0.001
siamensis vs. *muangfuangensis* sp. nov.	0.016	< 0.001	0.001	0.030							
somchanhae vs. *muangfuangensis* sp. nov.		<0.001	0.006								
sp. vs. *muangfuangensis* sp. nov.	< 0.001	< 0.001	< 0.001	< 0.001	0.001	< 0.001	0.016	0.001	0.013		< 0.001
vietnamensis vs. *muangfuangensis* sp. nov.	<0.001	0.00	<0.001	<0.001	<0.001	0.021	0.019	0.038	0.004		<0.001
somchanhae vs. *siamensis*		0.031					0.010		0.018		
sp. vs. *siamensis*	0.016	< 0.001	< 0.001	< 0.001		< 0.001	0.002	< 0.001	< 0.001	< 0.001	0.012
vietnamensis vs. *siamensis*	< 0.001	0.00	< 0.001		< 0.001		< 0.001	< 0.001	< 0.001	< 0.001	0.007
sp. vs. *somchanhae*	< 0.001	0.017	< 0.001	< 0.001	0.013	< 0.001		0.017		0.003	0.032
vietnamensis vs. *somchanhae*	< 0.001	0.00	< 0.001		< 0.001	0.003				0.013	0.038
vietnamensis vs. sp.		0.00		< 0.001		< 0.001					

Morphometric characters	SPLr.l	IFLr.l	MO	IOS	V	T4r.l
lao vs. *gialaiensis* sp. nov.		0.008	< 0.001			
minhlei vs. *gialaiensis* sp. nov.						
muangfuangensis sp. nov. vs. *gialaiensis* sp. nov.				< 0.001		
siamensis vs. *gialaiensis* sp. nov.				< 0.001		
somchanhae vs. *gialaiensis* sp. nov.					0.011	
sp. vs. *gialaiensis* sp. nov.						
vietnamensis vs. *gialaiensis* sp. nov.				0.041		
minhlei vs. *lao*		0.003	< 0.001			
muangfuangensis sp. nov. vs. *lao*		0.026	< 0.001			
siamensis vs. *lao*		0.007	< 0.001			
somchanhae vs. *lao*		< 0.001	< 0.001			
sp. vs. *lao*		0.002	< 0.001			
vietnamensis vs. *lao*	< 0.001	< 0.001	< 0.001		< 0.001	0.015
muangfuangensis sp. nov. vs. *minhlei*				0.004		
siamensis vs. *minhlei*				0.001		
somchanhae vs. *minhlei*					0.045	
sp. vs. *minhlei*						
vietnamensis vs. *minhlei*					0.038	
siamensis vs. *muangfuangensis* sp. nov.						

Morphometric characters	SPLr.l	IFLr.l	MO	IOS	V	T4r.l
somchanhae vs. *muangfuangensis* sp. nov.				0.010		
sp. vs. *muangfuangensis* sp. nov.						
vietnamensis vs. *muangfuangensis* sp. nov.					0.011	
somchanhae vs. *siamensis*		0.019			0.002	
sp. vs. *siamensis*					0.065	
vietnamensis vs. *siamensis*	0.022					0.035
sp. vs. *somchanhae*						
vietnamensis vs. *somchanhae*					< 0.001	
vietnamensis vs. sp.					< 0.001	
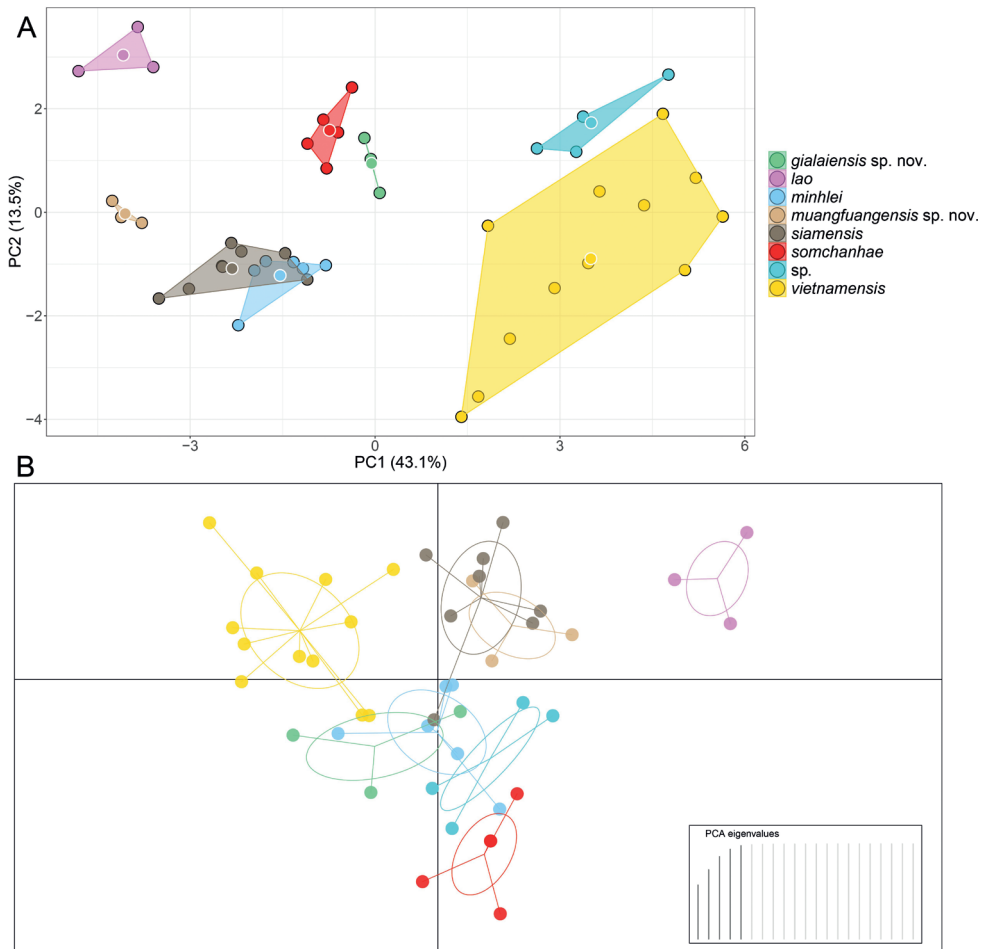
Figure 4. A principal component analysis (PCA) of *Dixonius* species showing their morphospatial relationships along the first two components based on normalized morphometric and meristic characters **B** discriminant analysis of principal components (DAPC) based on retention of the first five PCs with 67% inertia ellipsoids.
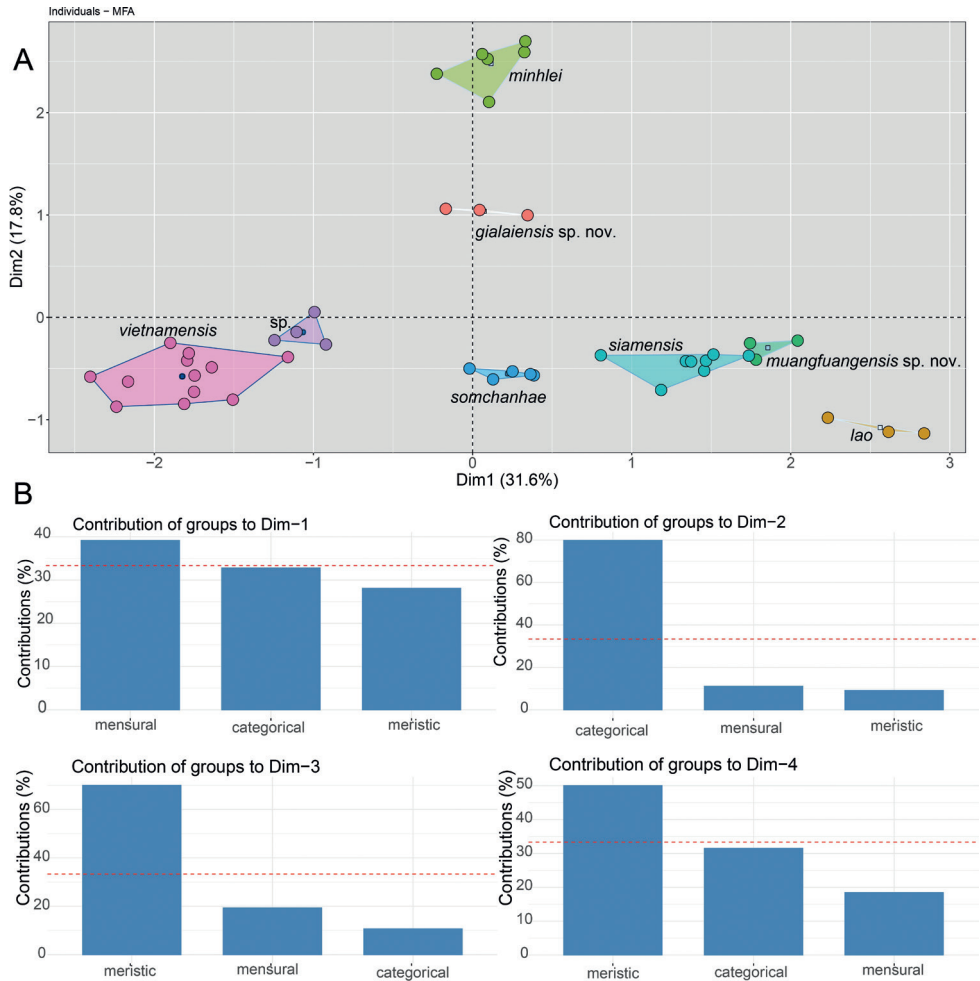
Figure 5. A MFA scatter plot showing the morphospatial relationships among the *Dixonius* species based on normalized morphometric, meristic, and color pattern characters **B** bar graphs showing the percent contribution of each data type to the overall variation in the data dimensions 1–4. The dashed red line in the bar graphs indicates the expected average value if the contributions of each data type were equal.

neck; prefrontal region concave; canthus rostralis rounded; snout elongate (ES/HL 0.37), rounded in dorsal profile; eye moderate size (ED/HL 0.25); ear opening oval, obliquely oriented, moderate in size; diameter of eye slightly smaller than eye to ear distance (ED/EE 0.88); rostral rectangular, partially divided dorsally by straight rostral groove, bordered posteriorly by large left and right supranasals, bordered laterally by first supralabials; external nares bordered anteriorly by rostral, dorsally by large supranasal, posteriorly by two smaller postnasals, bordered ventrally by first supralabial; 8,7 (R,L) rectangular supralabials extending to below and slightly past posterior margin of
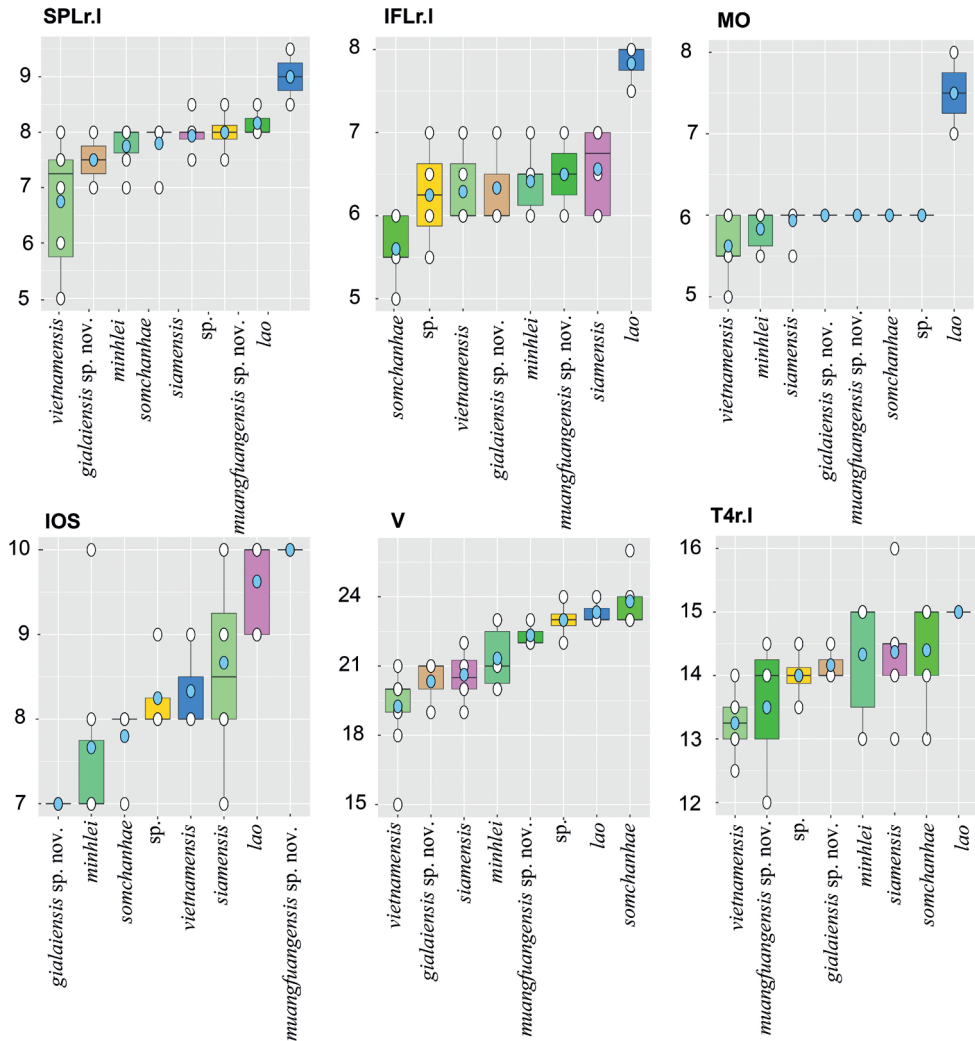
Figure 6. Boxplot comparisons of meristic characters among the *Dixonius* species where interspecific statistical differences were recovered (see Table 7). Pale blue circles are means and the black horizontal bars are medians.

eye, sixth in midorbital position; 6,6 (R,L), infralabials tapering smoothly to just below midpoint of eye, decreasing gradually in size; scales of rostrum and lores flat to domed, larger than granular scales on top of head and occiput; scales of occiput intermixed with distinct, small, conical tubercles; superciliaries elongate, largest anteriorly; mental triangular, bordered laterally by first infralabials and posteriorly by large left and right trapezoidal postmentals contacting medially for 60% of their length posterior to mental; gular and throat scales small, granular, grading anteriorly into slightly larger, flatter, smooth, imbricate, pectoral and ventral scales.

Body relatively short (AG/SVL 0.38); dorsal scales small, granular interspersed with larger, conical, regularly arranged, keeled tubercles; tubercles extend from top
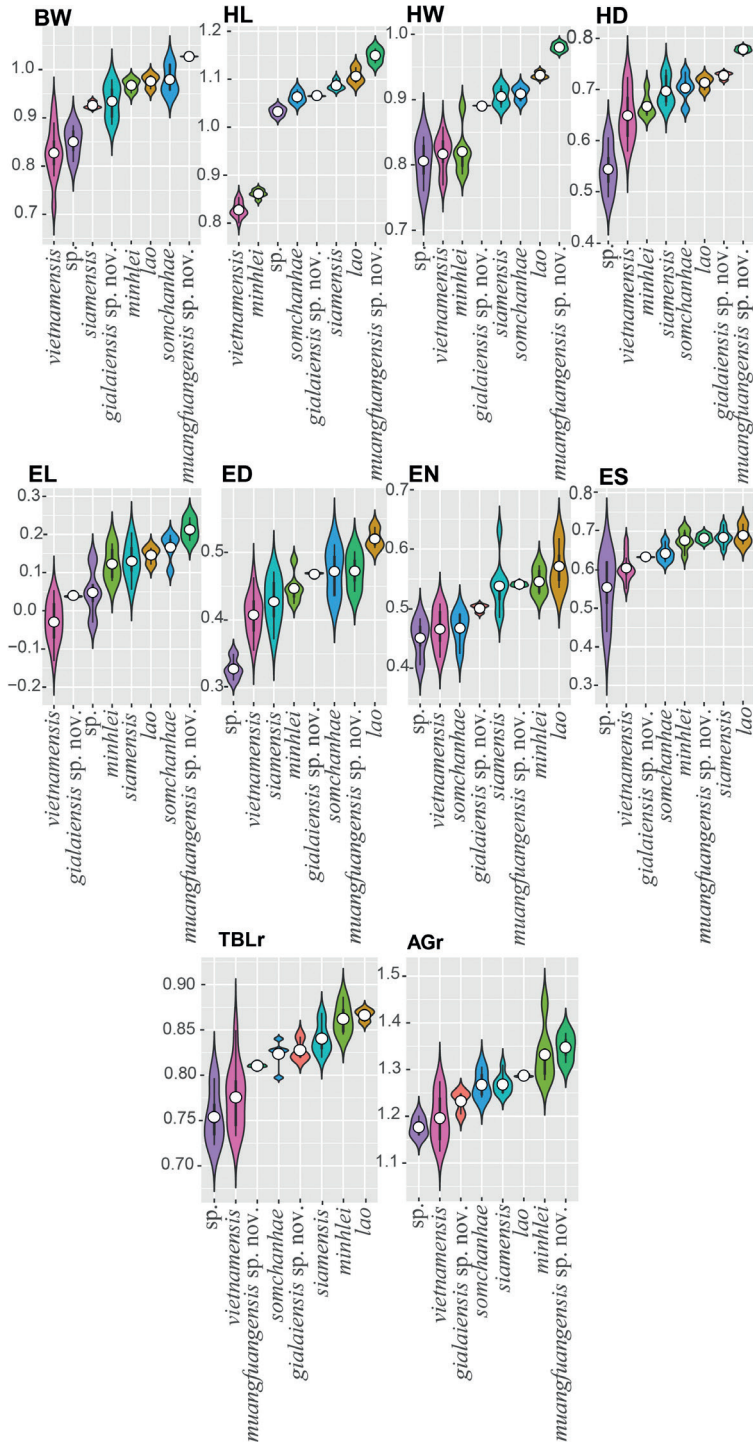
Figure 7. Violin plots of the normalized morphometric characters overlain with box plots showing the range, frequency, mean (white dot), and 50% quartile (black rectangle) of characters where interspecific statistical differences were recovered (see Table 7). New species in bold italics.

Figure 8. Dorsal views of *Dixonius gialaiensis* sp. nov. **A** adult male holotype VNUF R.2020.22 (Field no. GL02) **B** adult female paratype VNUF R.2020.33 (Field No. GL03) **C** juvenile male paratype VNUF R.2020.44 (Field No. GL04) in Chu Se Mountain Pass, Hbong Commune, Chu Se District, Gia Lai Province.

of head onto posterior haft of tail forming longitudinal rows, terminating at last portion of tail; smaller tubercles extend anteriorly onto nape and occiput, diminishing in size and distinction on top of head; 19 longitudinal rows of tubercles at midbody; 33 paravertebral scales, number of scales in a paravertebral row from first scale posterior to parietal scale to last scale at the level of vent opening; 23 paravertebral scales in a row between limb insertions; 21 flat, imbricate, ventral scales much larger than dorsal scales; 7 enlarge, pore-bearing, precloacal scales in an angular series; and no deep precloacal groove or depression.

Forelimbs moderate in stature, relatively short (FA/SVL 0.15); granular scales of forearm slightly larger than those on body, interspersed with small tubercles; hind limbs more robust than forelimbs, moderate in length (TBL/SVL 0.17), covered dorsally by granular scales interspersed with large, and small conical tubercles; ventral scales of thigh flat, imbricate, larger than dorsals; subtibial scales flat, imbricate; proximal femoral scales smaller than distal femorals; femoral pores absent; digits relatively long with 14 lamellae on fourth toe; and claws well developed.

Tail 108.4 mm in length, 4.5 mm in width at base, tapering to a point; dorsal scales of flat, square with conical, keeled tubercles in anterior part; median row of transversely expanded subcaudal scales, significantly larger than dorsal caudal scales on original portion; base of tail bearing hemipenal swellings; and postcloacal scales flat, imbricate.

Coloration in life (Fig. 8). Ground color of dorsal head and dorsum grey brown with rounded black-brown blotches, decreasing gradually in size from head to body; canthal stripe continues behind orbit to back of head; dark bars on the lips; uneven light spots running from postorbital along the flanks to tip tail; upper surface of fore- and hindlimbs uniformly light grey with black-brown spots; dorsum of tail covered with some small rounded black-brown blotches; ventral surface beige uniformly as the belly and the throat.

Variation (Fig. 8). The female paratype (VNUF R.2020.33) generally has more dark brown blotches on head and dorsum, and uniformly black on the new regenerated tail. The dorsum of the of head and body of the juvenile male paratype (VNUF R.2020.44) pale brown with pale-colored blotches on granulose skin arranged along its sides extending from the flanks to the tail tip. Further measurements are summarized in Tables 2–4, Suppl. material 1: table S1.

Distribution. *Dixonius gialaiensis* sp. nov. currently is only known from the type locality of Chu Se Mountain Pass, H'Bong Commune, Chu Se District, Gia Lai Province, Central Highlands, Vietnam (Fig. 1).

Natural history. The specimens were found at night, between 19:45 and 21:00 h, on the ground in an area along the National Highway 25. The surrounding habitat was secondary montane forest with woody trees. The temperature and humidity were approximately 32.6 °C and 57% (Fig. 9).

Etymology. The new species is named after the type locality of Gia Lai Province, Central Highlands, Vietnam.

Comparisons. *Dixonius gialaiensis* sp. nov. is the sister species to *D. minhlei* (Fig. 2) from which it differs by an uncorrected pairwise sequence divergence of 3.60% (Table 4). It is differentiated from it morphologically by having a significantly higher

Figure 9. Habitat of *Dixonius gialaiensis* sp. nov. HBong Commune, Chu Se District, Gia Lai Province, Central Highlands, Vietnam.

mean number of head length (HL), head width (HW), and axilla to groin length (AG). In addition, it differs from *D. minhlei* in color pattern (grey-brown dorsum with more round black-brown blotches versus olive gray dorsum with round brownish olive blotches). Statistically significant and discrete categorical differences between *Dixonius gialaiensis* sp. nov. and all other species and populations are presented in Tables 5–7.

Dixonius muangfuangensis sp. nov.

https://zoobank.org/A447EC01-F653-4FE5-A616-5FBD25F027C6
Fig. 10
Muangfuang leaf-toed gecko

Material examined. *Holotype.* Adult male, VNUF R.2020.42 (Field no. MF.02) in Sinxay Temple, Nadan Village, Muangfuang District, Vientiane Province, Central Laos (18°32'52"N, 101°58'31"E; 276 m a.s.l.), collected by Saly Sitthivong and Thuong Huyen Nguyen on 05 December 2020. *Paratypes.* NUOL R.2022.01 (Field no. MF. 01), juvenile male, and VNUF R.2020.52 (Field no. MF. 03), adult female; the same data as given for the holotype.

  Diagnosis. *Dixonius muangfuangensis* sp. nov. can be separated from all other species of *Dixonius* by possessing the unique combination of having a maximum SVL of 56.7 mm; 21–23 longitudinal rows of dorsal tubercles at midbody; 20 or 21 longitudinal rows of ventrals across the abdomen; 7 or 8 supralabials, sixth in at midorbital position; 6 or 7 infralabials; 7 interorbital scales; 7 or 8 precloacal pores in males, femoral pores lacking; precloacal and femoral pores absent in female; 15 lamellae on fourth toe;

dorsum olive grey color with numerous small and irregular black blotches; head with brown spots; light spots irregularly arranged from the back of the head to base of tail; lips with dark bars; two regularly disposed whitish tubercles on each side on each side. These characters are scored across all *Dixonius* species from Vietnam and Laos in Tables 6, 7.

Description of the holotype. Adult male, SVL 55.6 mm; head moderate in length (HL/SVL 0.28), wide (HW/HL 0.71), depressed (HD/HL 0.45), distinct from neck; prefrontal region concave; canthus rostralis rounded; snout elongate (ES/HL 0.39), rounded in dorsal profile; eye moderate size (ED/HL 0.20); ear opening oval, obliquely oriented, moderate in size; diameter of eye much smaller than eye to ear distance (ED/EE 0.59); rostral rectangular, partially divided dorsally by straight rostral groove, bordered posteriorly by large left and right supranasals, bordered laterally by first supralabials; external nares bordered anteriorly by rostral, dorsally by large supranasal, posteriorly by two smaller postnasals, bordered ventrally by first supralabial; 8,8 (R,L) rectangular supralabials extending to below midpoint of eye, sixth in midorbital position; 7,7 (R,L), infralabials tapering smoothly to be just slightly past posterior below midpoint of eye, decreasing gradually in size; scales of rostrum and lores flat to domed, larger than granular scales on top of head and occiput; scales of occiput intermixed with distinct, small, conical tubercles; superciliaries elongate, largest anteriorly; mental triangular, bordered laterally by first infralabials and posteriorly by large left and right parallelogram postmentals contacting medially for 60% of their length posterior to mental; gular and throat scales small, granular, grading anteriorly into slightly smaller, flatter, smooth, imbricate, pectoral and ventral scales.

Body relatively short (AG/SVL 0.42) with well-defined ventrolateral folds; dorsal scales small, granular interspersed with moderate, conical, regularly arranged, keeled tubercles; tubercles extend from top of head onto interior haft of tail forming longitudinal rows, terminating at regenerated portion of tail; smaller tubercles extend anteriorly onto nape and occiput, diminishing in size and distinction on top of head; 23 longitudinal rows of tubercles at midbody; 45 paravertebral scales, number of scales in a paravertebral row from first scale posterior to parietal scale to last scale at the level of vent opening; 24 paravertebral scales in a row between limb insertions; 20 flat, imbricate, ventral scales much larger than dorsal scales; 8 enlarge, pore-bearing, precloacal scales in an angular series; and no deep precloacal groove or depression.

Forelimbs moderate in stature, relatively short (FA/SVL 0.12); granular scales of forearm slightly larger than those on body, interspersed with small tubercles; hind limbs more robust than forelimbs, moderate in length (TBL/SVL 0.13), covered dorsally by granular scales interspersed with large, and small conical tubercles; ventral scales of thigh flat, imbricate, larger than dorsals; subtibial scales flat, imbricate; proximal femoral scales smaller than distal femorals; femoral pores absent; digits relatively long with 15 lamellae on fourth toe; and claws well developed.

Tail 37.8 mm in length, first 17.1 mm original, 6.1 mm in width at base, tapering to a point; dorsal scales of flat, square with conical, keeled tubercles, regenerated portion covered with small, smooth subcircular scales; median row of transversely expanded subcaudal scales, significantly larger than dorsal caudal scales on original portion; base of tail bearing hemipenal swellings; and postcloacal scales flat, imbricate.

Figure 10. View of *Dixonius muangfuangensis* sp. nov. **A** adult male holotype VNUF R.2020.42 (Field no. MF.02) **B** adult female paratype VNUF R.2020.52 (Field no. MF. 03) **C** juvenile male paratype NUOL R.2022.01 (Field no. MF. 01) in Nadan Village, Muangfuang District, Vientiane Province, Central Laos.

Figure 11. Habitat of *Dixonius muangfuangensis* sp. nov. Nadan Village, Muangfuang District, Vientiane Province, Central Laos.

Coloration in life (Fig. 10). Ground color of dorsal head and dorsum dark grey with numerous small and irregular black blotches; lips with dark bars; two regularly disposed whitish tubercles on each side on each side running from postorbital along the flanks to tail, terminating at regenerated portion of tail; upper surface of fore and hind limbs uniformly dark brown with round black-brown spots; dorsum of tail covered with some large black-brown blotches; ventral surface beige uniformly as the belly and the throat.

Variation (Fig. 10). The female paratype (VNUF R.2020.52) generally matches that of the holotype in all characteristics. The juvenile male paratype (NUOL R.2022.01) has fewer black blotches on head and dorsum and two regularly disposed whitish tubercles on each side on each side of the head extending from the postorbital region, along the flanks, to the tail tip. Further measurements are summarized in Tables 2–4 and Suppl. material 1: table S2.

Distribution. *Dixonius muangfuangensis* sp. nov. currently is only known from the type locality of Nadan Village, Muangfuang District, Vientiane Province, Central Laos (Fig. 1).

Etymology. The specific epithet of the new species refers to the type locality of the new species in Muangfuang District, Vientiane Province, Central Laos.

Natural history. The type series was collected between 19:10 and 19:30 h, on the ground inside Sinxay Temple, at an elevation of 276 m a.s.l. The surrounding habitat was disturbed lowland karst forest (Fig. 11).

Comparisons. *Dixonius muangfuangensis* sp. nov. is the sister species to *D. lao* (Fig. 2) from which it differs by an uncorrected pairwise sequence divergence of 3.10% (Table 4). It is differentiated morphologically by having a significantly higher mean number of head length (HL), infralabials (IFL), and numbers of supralabial at midorbital position (MO). In addition, it differs from *D. lao* in dorsal pattern (dorsal pebble brown versus dorsal dark gray with black blotches). Statistically significant and discrete categorical differences between *Dixonius muangfuangensis* sp. nov. and all other species and populations are presented in Tables 5–7.

Discussion

Morphological comparisons indicated that *Dixonius gialaiensis* sp. nov. is most similar to its sister species *D. minhlei*, but can be differentiated from the latter species by the number of dorsal tubercle scale rows and differences in color pattern. The results of the molecular analysis show the uncorrected pairwise sequence divergence between the two taxa is 3.60%. Additionally, the two species are widely separated geographically being in different mountain systems and separated by the Dong Nai River system (Fig. 1). Collectively, these data suggest these are separate and distinct species.

Dixonius gialaiensis sp. nov. was discovered in a protected forest near the National Highway 25. The construction of new infrastructure at this site strongly impacts the habitat of *D. gialaiensis* sp. nov., including range fragmentation and forest degradation. Further investigations on conservation status is urgently required to develop effective conservation measures.

Dixonius muangfuangensis sp. nov. is most closely related to *D. lao*, but can be distinguished from it by head shape and color pattern differences. The molecular analysis indicated these two species differ by a 3.1% uncorrected pairwise genetic distance. In addition, the two species evolved separately in geographically isolated regions. The type locality of *D. muangfuangensis* sp. nov. is approximately 500 km south of the type locality of *D. lao* and the type localities are separated by the Nam Ngiap and Xebangfai river network systems (Fig. 1).

The BEAST analysis indicates that the divergence between *Dixonius gialaiensis* sp. nov. and *D. minhlei* and that between *D. muangfuangensis* sp. nov. and *D. lao* may have been the result of cyclical climatic events during the recent interglacial periods of the Pliocene as noted for several other Indochinese species (see Grismer and Grismer 2017 and references therein). *D. muangfuangensis* sp. nov. and *D. lao* diverged from one another at approximately 3.47 mya. Relatively soon after, at approximately 3.19 mya, *Dixonius gialaiensis* sp. nov. and *D. minhlei* separated from one another, thus allowing sufficient time for them to evolve significant differences between them in a number of characteristics. During this time period, the formation of separate karstic habitats and granitic mountains and hills may have prevented gene flow between these populations, placing each species on separate evolutionary trajectories (Grismer and Grismer 2017).

Acknowledgements

References

Barraclough TG, Birky Jr CW, Burt A (2003) Diversification in sexual and asexual organisms. Evolution; International Journal of Organic Evolution 57: 2166–2172. https://doi.org/10.1554/02-339

Bauer AM, Branch WR, Good DA (1997) The taxonomy of the southern African leaf-toed geckos (Squamata: Gekkonidae), with a review of old world. Proceedings of the California Academy of Sciences 49(14): 447–497.

Bauer AM, Sumontha M, Grossmann W, Pauwels OSG, Vogel G (2004) A new species of *Dixonius* (Squamata: Gekkonidae) from Kanchanaburi Province, western Thailand. Current Herpetology 23(1): 17–26. https://doi.org/10.5358/hsj.23.17

Botov A, Phung TM, Nguyen TQ, Bauer AM, Brennan IG, Ziegler T (2015) A new species of *Dixonius* (Squamata: Gekkonidae) from Phu Quy Island, Vietnam. Zootaxa 4040(1): 48–58. https://doi.org/10.11646/zootaxa.4040.1.4

Bouckaert RR, Drummond AJ (2017) bModelTest: Bayesian phylogenetic site model averaging and model comparison. BMC Evolutionary Biology 17(1): 1–42. https://doi.org/10.1186/s12862-017-0890-6

Boulenger GA (1898) Third report on additions to the lizard collection in the Natural History Museum. Proceedings of the Zoological Society of London 1898(4): 912–923. https://doi.org/10.1111/j.1096-3642.1898.tb03194.x [pls LV–LVII.]

Chan KO, Grismer LL (2022) GroupStruct: An R package for allometric size correction. Zootaxa 5124(4): 471–482. https://doi.org/10.11646/zootaxa.5124.4.4

Das I (2004) A new species of *Dixonius* (Sauria: Gekkonidae) from southern Vietnam. The Raffles Bulletin of Zoology 52(2): 629–634. https://doi.org/10.5358/hsj.23.63

De Queiroz K (2007) Species concepts and species delimitation. Systematic Biology 56(6): 879–886. https://doi.org/10.1080/10635150701701083

Drummond AJ, Suchard MA, Xie D, Rambaut A (2012) Bayesian Phylogenetics with BEAUti and BEAST 1.7. Molecular Biology and Evolution 29(8): 1969–1973. https://doi.org/10.1093/molbev/mss075

Frost DR, Hillis DM (1990) Species in concept and practice: Herpetological application. Herpetologica 46: 87–104.

Frost DR, Kluge AG (1994) A consideration of the epistemology in systematic biology, with special reference to species. Cladistics 10(3): 259–294. https://doi.org/10.1111/j.1096-0031.1994.tb00178.x

Gamble T, Greenbaum E, Jackman TR, Bauer AM (2015) Into the light: Diurnality has evolved multiple times in geckos. Biological Journal of the Linnean Society. Linnean Society of London 115(4): 896–910. https://doi.org/10.1111/bij.12536

Grismer LL, Grismer JL (2017) A re-evaluation of the phylogenetic relationships of the *Cyrtodactylus condorensis* group (Squamata; Gekkonidae) and a suggested protocol for the characterization of rock-dwelling ecomorphology in *Cyrtodactylus*. Zootaxa 4300(4): 486–504. https://doi.org/10.11646/zootaxa.4300.4.2

Hillis DM (2019) Species delimitation in herpetology. Journal of Herpetology 53(1): 3–12. https://doi.org/10.1670/18-123

Hoang DT, Chernomor O, von Haeseler A, Minh BQ, Vinh LS (2018) UFBoot2: Improving the ultrafast bootstrap approximation. Molecular Biology and Evolution 35(2): 518–522. https://doi.org/10.1093/molbev/msx281

Huelsenbeck JP, Ronquist F, Nielsen R, Bollback JP (2001) Bayesian inference of phylogeny and its impact on evolutionary biology. Science 294(5550): 2310–2314. https://doi.org/10.1126/science.1065889

Husson F, Josse J, Le S, Mazet J (2017) FactoMine R: Exploratory Data Analysis and Data Mining. R package version 1.36.

Jombart T, Devillard S, Balloux F (2010) Discriminant analysis of principal components: A new method for the analysis of genetically structured populations. BMC Genetics 11(1): 1–15. https://doi.org/10.1186/1471-2156-11-94

Kalyaanamoorthy S, Minh BQ, Wong TK, von Haeseler A, Jermiin LS (2017) ModelFinder: Fast model selection for accurate phylogenetic estimates. Nature Methods 14(6): 587–589. https://doi.org/10.1038/nmeth.4285

Kassambara A, Mundt F (2017) factoextra: Extract and Visualize the Result of Multivariate Data Analyses. R package version 1.0.5.999.

Kumar S, Stecher G, Tamura K (2016) MEGA7: Molecular evolutionary genetics analysis version 7.0 for bigger datasets. Molecular Biology and Evolution 33(7): 1870–1874. https://doi.org/10.1093/molbev/msw054

Lleonart J, Salat J, Torres GJ (2000) Removing allometric effects of body size in morphological analysis. Journal of Theoretical Biology 205(1): 85–93. https://doi.org/10.1006/jtbi.2000.2043

Macey JR, Larson A, Ananjeva NB, Fang Z, Papenfuss TJ (1997) Two novel gene orders and the role of light-strand replication in rearrangement of the vertebrate mitochondrial genome. Molecular Biology and Evolution 14(1): 91–104. https://doi.org/10.1093/oxfordjournals.molbev.a025706

McCoy MW, Bolker BM, Osenberg CW, Miner BG, Vonesh JR (2006) Size correction: Comparing morphological traits among populations and environments. Oecologia 148(4): 547–554. https://doi.org/10.1007/s00442-006-0403-6

Miller MA, Pfeiffer W, Schwartz T (2010) Creating the CIPRES Science Gateway for inference of large phylogenetic trees. Proceedings of the Gateway Computing Environments Workshop (GCE), New Orleans, Louisiana, 14 November 2010, 8 pp. https://doi.org/10.1109/GCE.2010.5676129

Minh Q, Nguyen MAT, von Haeseler A (2013) Ultrafast approximation for phylogenetic bootstrap. Molecular Biology and Evolution 30(5): 1188–1195. https://doi.org/10.1093/molbev/mst024

Ngo VT, Ziegler T (2009) A new species of *Dixonius* from Nui Chua National Park, Ninh Thuan Province, southern Vietnam (Squamata, Gekkonidae). Zoosystematics and Evolution 85(1): 117–125. https://doi.org/10.1002/zoos.200800018

Nguyen LT, Schmidt HA, von Haeseler A, Minh BQ (2015) IQ-TREE: A fast and effective stochastic algorithm for estimating maximum likelihood phylogenies. Molecular Biology and Evolution 32(1): 268–274. https://doi.org/10.1093/molbev/msu300

Nguyen TH, Sitthivong S, Ngo HT, Luu VQ, Nguyen TQ, Le MD, Ziegler T (2020) A new species of *Dixonius* (Squamata: Gekkonidae) from the karst forest of Khammouane Province, central Laos. Zootaxa 4759(4): 530–542. https://doi.org/10.11646/zootaxa.4759.4.4

Nguyen TH, Luu VQ, Sitthivong S, Ngo HT, Nguyen TQ, Le MD, Ziegler T (2021) A new species of *Dixonius* (Squamata: Gekkonidae) from Vientiane Capital, Laos. Zootaxa 4965(2): 351–362. https://doi.org/10.11646/zootaxa.4965.2.8

Pagès J (2015) Multiple Factor Analysis by Example Using R. CRC Press, New York, 272 pp. https://doi.org/10.1201/b17700

Pauwels OSG, Panitvong N, Kunya K, Sumontha M (2021) A new sandstone-dwelling leaf- toed gecko (Gekkonidae: *Dixonius mekongensis*) from the Thai-Lao border. Zootaxa 4969(3): 526–538. https://doi.org/10.11646/zootaxa.4969.3.5

R Core Team (2021) R: A language and environment for statistical computing. R Foundation for Statistical Computing. Vienna. 2018. http://www.R-project.org [Accessed 1 December 2022]

Rambaut A, Drummond AJ (2013) TreeAnnotator. Version 1.7.3 MCMC Output Analysis. https://beast. community/treeannotator [Accessed 15 January 2023]

Rambaut A, Suchard MA, Xie D, Drummond AJ (2014) Tracer. Version 1.7. http://tree.bio.ed.ac.uk/ software/tracer/ [Accessed 15 January 2023]

Reist JD (1986) An empirical evaluation of coefficients used in residual and allometric adjustment of size covariation. Canadian Journal of Zoology 64(6): 1363–1368. https://doi.org/10.1139/z86-203

Ronquist F, Teslenko M, van der Mark P, Ayres DL, Darling A, Höhna S, Larget B, Liu L, Suchard MA, Huelsenbeck JP (2012) MrBayes 3.2: Efficient Bayesian phylogenetic inference and model choice across a large model space. Systematic Biology 61(3): 539–542. https://doi.org/10.1093/sysbio/sys029

Taylor EH (1962) New oriental reptiles. The University of Kansas Science Bulletin 43: 209–263. https://doi.org/10.5962/bhl.part.13346

Thorpe RS (1975) Quantitative handling of characters useful in snake systematics with particular reference to interspecific variation in the Ringed Snake *Natrix natrix* (L.). Biologi-

cal Journal of the Linnean Society. Linnean Society of London 7(1): 27–43. https://doi. org/10.1111/j.1095-8312.1975.tb00732.x

Thorpe RS (1983) A review of the numerical methods for recognizing and analyzing racial differentiation. In: Felsenstein J (Ed.) Numerical Taxonomy. NATO ASI Series (Series G: Ecological Sciences) (Vol. 1). Springer-Verlag, Berlin, 404–423. https://doi.org/10.1007/978-3-642-69024-2_43

Trifinopoulos J, Nguyen LT, von Haeseler A, Minh BQ (2016) W-IQ-TREE: A fast online phylogenetic tool for maximum likelihood analysis. Nucleic Acids Research 44(W1): W232–W235. https://doi.org/10.1093/nar/gkw256

Turan C (1999) A note on the examination of morphometric differentiation among fish populations: The Truss System. Turkish Journal of Zoology 23: 259–263.

Uetz P, Freed P, Aguilar R, Reyes F, Hošek J [Eds] (2022) The Reptile Database. http://www. reptile-database.org [Accessed 14 January 2023]

Wilcox TP, Zwickl DJ, Heath TA, Hillis DM (2002) Phylogenetic relationships of the Dwarf Boas and a comparison of Bayesian and bootstrap measures of phylogenetic support. Molecular Phylogenetics and Evolution 25(2): 361–371. https://doi.org/10.1016/S1055-7903(02)00244-0

Ziegler T, Botov A, Nguyen TT, Bauer AM, Brennan IG, Ngo HT, Nguyen TQ (2016) First molecular verification of *Dixonius vietnamensis* Das, 2004 (Squamata: Gekkonidae) with the description of a new species from Vinh Cuu Nature Reserve, Dong Nai Province, Vietnam. Zootaxa 4136(3): 553–566. https://doi.org/10.11646/zootaxa.4136.3.7

Supplementary material 1

Measurements and morphological characters of the type series of *Dixonius gialaiensis* sp. nov.

Authors: Vinh Quang Luu, Thuong Huyen Nguyen, Minh Duc Le, Jesse L. Grismer, Hong Bich Ha, Saly Sitthivong, Tuoi Thi Hoang, L. Lee Grismer

Data type: tables (Excel spreadsheet)

Explanation note: table S1: Measurements (in mm) and morphological characters of the type series of *Dixonius gialaiensis* sp. nov. (for abbreviations see Material and methods). Measurements taken on right side; FA is given in the left side; SPL/IFL/T4 given in right/ left order; -absence; * tail regenerated; table S2: Measurements (in mm) and morphological characters of the type series of *Dixonius muangfuangensis* sp. nov. (for abbreviations see material and methods). Measurements taken on right side; FA and T4 are given in the left side; SPL/IFL given in right/ left order; -absence, * tail regenerated; ** tail lost.

Link: https://doi.org/10.3897/zookeys.1163.101230.suppl1